



Semnan University

Mechanics of Advanced Composite Structures

journal homepage: <http://MACS.journals.semnan.ac.ir>

A New Three-Dimensional Refined Higher-Order Theory for Free Vibration Analysis of Composite Circular Cylindrical Shells

A. Davar*, R. Kohandani, H.M. Panahiha

Composite Research Centre, Malek Ashtar University of Technology, Lavizan, Tehran, Iran

PAPER INFO

Paper history:

Received 2018-05-18
 Received in revised form
 2018-08-27
 Accepted 2019-04-25

Keywords:

Free vibration
 Higher-order shear deformation
 theory
 Trapezoidal shape factor
 Circular cylindrical shells
 Composite

ABSTRACT

A new closed form formulation of three-dimensional (3-D) refined higher-order shell theory (RHOST) to analyze the free vibration of composite circular cylindrical shells has been presented in this article. The shell is considered to be laminated with orthotropic layers and simply supported boundary conditions. The proposed theory is used to investigate the effects of the in-plane and rotary inertias as well as transverse normal and shear strains on the dynamic response of thick composite cylindrical shells. The trapezoidal shape factor of the shell element is incorporated to obtain accurate stress-resultants. Using Hamilton's principle, the equations of motion are obtained and solved in terms of the Galerkin method. Numerical results for the natural frequencies are verified by making comparison with the 3-D exact elasticity iterative solutions in the literature. In addition, the validity of the results is further verified by ABAQUS. According to the results, for thick composite cylinders with large length-to-radius and orthotropic ratios, through thickness exact integration yields accurate stress-resultants for proper prediction of the natural frequencies.

© 2019 Published by Semnan University Press. All rights reserved.

1. Introduction

Cylindrical shells are widely used in many industries such as gas pipelines, petrol conveying. Also, cylindrical structures are common in modern industries such as aerospace, aircraft and marine structures. Based on classical shells theories, which are based on Kirchhoff-Love's hypothesis, many studies have been performed on shells [1]. Although classical shell theories ignore the transverse stress and strain components for easy calculation, this omission gives inadequate results for the analysis of thick cylindrical shells [1]. Some research studies are presented in the literature that investigate the effects of shear deformation for dynamic response of composite cylindrical shells [2]. Leissa [3] has summarized many studies in the state-of-the-art in his research work. According to these research studies, the effect of shear deformation can become

significant for small length-to-thickness or radius-to-thickness ratios. Bhimaraddi [4], developed a two-dimensional higher-order shell theory to investigate the dynamic response of composite circular cylindrical shell and the traction free condition is assumed for inner and outer surfaces of the shell. Reddy and Liu [5] presented a two-dimensional (2-D) higher-order theory for laminated elastic shells. The theory accounts for parabolic distribution of the transverse shear strains through thickness of the shell and tangential stress-free boundary conditions on the boundary surface of the shell.

The 2-D higher-order shell theories consider the effects of shear deformation and rotary inertia and they are more useful than the thin shell theories for the analysis of moderately thick shell structures. In order to analyze the thick shells, 2-D higher-order shell theories are not adequate especially in the case

*Corresponding author: Tel: +982122945141, Fax: +982122935341
 E-mail address: davar78@gmail.com

of higher frequencies. In order to analyze the thick shells, the transverse normal stress and strain components which are neglected in the 2-D higher-order shell theories, should be accounted for in the analysis which is based on three-dimensional (3-D) shell theories.

Due to accounting all the transverse stress and strain components (which are ignored in the 2-D higher-order shell theories), the dynamic analysis of circular cylindrical shells on the basis of the governing equations of the 3-D elasticity attracted the attention of researchers. In recent years, by refinement of thick-shell theories, some new 3-D shell theories for the case of homogeneous cylindrical shells were investigated [6-8] as reviewed by Qatu [9]. Khalili et al. [10] investigated dynamic responses of free vibration analysis of homogenous isotropic circular cylindrical shells based on a new 3-D refined higher-order theory.

In the case of multi-layered anisotropic composite shells, the effects of transverse shear deformation are more significant as compared to isotropic shells. Hence, the dynamic behavior of composite shells is more complicated than isotropic ones. Because of this complexity, accurate results for dynamic response of composite shells need three-dimensional modeling instead of two-dimensional one especially for analysis of thick shells where transverse normal and shear strains become more significant. Rogers and Knight [11] have formulated a linear higher-order finite element to analyze an axisymmetric composite structure. A higher-order theory for the analysis of composite cylindrical shells was proposed by Murthy et al. [12] by expanding the displacement variables in the form of power series and retaining a finite number of terms. As a result, the formulation allows for arbitrary variation of in-plane displacement. Three-dimensional elasticity solutions were presented for the vibration of cross-ply laminated simply supported cylindrical shells by Ye and Soldatos [13]. They used an iterative procedure and after a few iterations, they obtained the exact values for the natural frequencies. Natural frequencies and their mode shapes of some homogeneous orthotropic cross-ply cylinders were investigated. Kant and Menon [14] presented a higher-order refined theory for composite and sandwich cylindrical shells with finite number of elements which is suitable for the analysis of thin and moderately thick anisotropic laminated cylindrical shells. Timarci and Soldatos [15] presented comparative dynamic research studies for symmetric cross-ply cylindrical shells using unified shear-deformable shell theory.

Most of the research studies for higher-order shear deformation theories that include shear deformation and rotary inertia, failed to consider the $(1 + z/R)$ terms (trapezoidal shape factor) that is considered due to the fact that the stresses over the thickness of the shell have to be integrated on a trapezoidal cross-section of a shell element to obtain the accurate stress resultants. As shown in Fig. 1, an element of the shell section is presented. As it can be seen, taking into account the large shape trapezoidal coefficient (including $1+z/R$ terms), instead of the rectangular shape (excluding $1+z/R$ terms), is closer to reality, and therefore precision of the integration increased for calculating the stress resultants in the axial direction.

Chang [16] and Leissa and Chang [17] considered this term but by neglecting the terms beyond the order of h/R . For the first time, Qatu [18] utilized the $(1 + z/R)$ shape factor within the framework of first order shear deformation theory (FSDT) to analyze the free vibration of laminated deep thick shells. Lam and Qian [19] developed a theoretical analysis and analytical solution for vibrations of thick symmetric angle-ply laminated composite shells considering trapezoidal shape factor $(1 + z/R)$. Icardi and Ruotolo [20] presented a multi-layered model based on a second-order expansion of the $(1 + z/R)$ terms. They presented some numerical results concerning eigenfrequencies and stress distributions across the thickness of simply supported, cross-ply cylindrical shells. As a result, incorporation of the second-order expansion of the $(1 + z/R)$ terms appears to be suited for technical purposes, as it can improve the accuracy for predicting the overall and local behavior of rather thick shells. Other research studies which incorporate the $(1 + z/R)$ terms in the static and dynamic analysis of thick laminated cylindrical shells are presented in Refs. [21-25]. In these studies, the most popular procedures are finite element method, Ritz method and the series solution method.

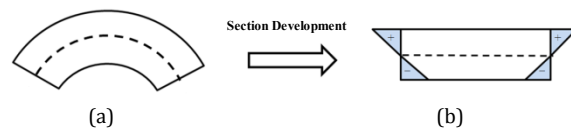


Fig. 1. (a) Circumferential cross-section of a thick cylinder for integrating stress resultants in axial direction; (b) Regions shown by + and - signs indicate the area differences between the assumed (rectangular and trapezoidal) developed shapes of the cross-section.

The main purpose of this work is to investigate a closed form solution of the free vibration of simply supported-simply supported (SS-SS) composite laminated circular cylindrical shells using a three-dimensional (3-D) refined higher-order shell theory (RHOST). The effects of the in-plane and rotary inertias and transverse normal and shear strains on the dynamic response of composite cylindrical shells have been investigated. Due to the fact that the stresses over the thickness of the shell are to be integrated on trapezoidal-like cross section of a shell element, trapezoidal shape factor $(1 + z/R)$ is also considered for the first time in the framework of the present RHOST. The present work is an extension of the first author earlier research on free vibrations of thick homogenous isotropic cylinders [10] to multi-layered thick composite cylinders. The advantage of the present RHOST is that no iterative procedure like those used for example in Refs. [1] and [13] is required for calculating the natural frequencies and hence, less CPU-time is consumed and this would be useful especially in optimization processes where frequency should be calculated several times.

2. Formulation

A circular cylindrical shell as shown in Fig. 2 is considered with radius R , thickness h and length L . The displacement components in the axial, tangential and radial directions are u , v and w , respectively and the reference coordinate system (x, φ, z) , is placed on the middle surface of the cylindrical shell.

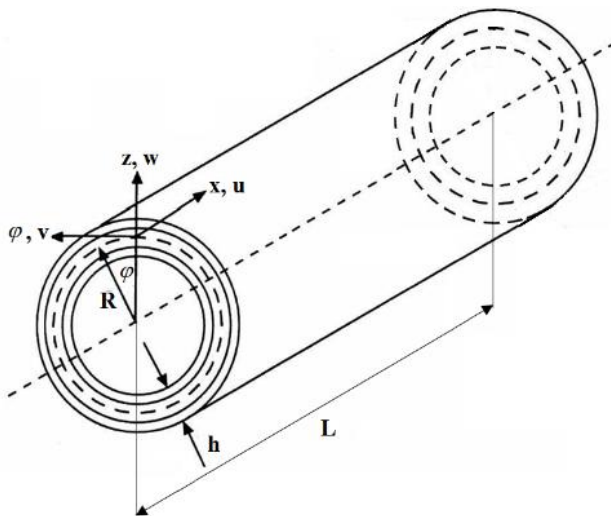


Fig. 2. A circular cylindrical shell with the reference coordinate system

In order to formulate a 3-D elasticity problem, the Taylor's series expansion is used and the following equations are obtained by expanding the displacement components $u(x, \varphi, z, t)$, $v(x, \varphi, z, t)$ and $w(x, \varphi, z, t)$ in terms of thickness coordinate z of any point of shell space [10]:

$$\begin{aligned}
 u(x, \varphi, z, t) &= u_0(x, \varphi, t) + z\theta_x(x, \varphi, t) + z^2u_0^*(x, \varphi, t) + z^3\theta_x^*(x, \varphi, t) \\
 v(x, \varphi, z, t) &= (1 + \gamma_0 z / R)v_0(x, \varphi, t) + z\theta_\varphi(x, \varphi, t) + z^2v_0^*(x, \varphi, t) + z^3\theta_\varphi^*(x, \varphi, t) \\
 w(x, \varphi, z, t) &= w_0(x, \varphi, t) + z\theta_z(x, \varphi, t) + z^2w_0^*(x, \varphi, t) + z^3\theta_z^*(x, \varphi, t)
 \end{aligned}
 \tag{1}$$

The terms u , v and w are the displacements components and t is the time. It should be noted that 12 displacement parameters are presented in Eq. (1) as a higher-order displacement field. By setting the coefficient γ_0 equal to 1 in Eq. (1), the trapezoidal shape factor of the cylindrical shell is applied in the equilibrium equations and the HOST12 theory ($\gamma_0 = 0$) is refined to RHOST12. u_0 , v_0 are the in-plane displacements of the cylindrical shell and w_0 is the transverse displacement of a point (x, φ) on the shell middle surface. θ_x , θ_φ are the rotation functions of the normal to the shells middle surface about φ - and x - axis, respectively. u_0^* , v_0^* , w_0^* , θ_x^* , θ_φ^* and θ_z^* are the higher-order terms in the Taylor's series expansion that represent higher-order transverse deformation modes. For the first-order shear deformation theory, only u_0 , v_0 , w_0 , θ_x and θ_φ are considered as displacement field. The general strain-displacement relations in the cylindrical coordinate system according to linear theory of elasticity for circular cylindrical shells are defined as follow [10]:

$$\begin{aligned}
 \varepsilon_x &= \frac{\partial u}{\partial x} \\
 \varepsilon_\varphi &= \frac{1}{1 + \gamma_0 z / R} \left(\frac{1}{R} \frac{\partial v}{\partial \varphi} + \frac{w}{R} \right) \\
 \varepsilon_z &= \frac{\partial w}{\partial z} \\
 \gamma_{x\varphi} &= \frac{1}{1 + \gamma_0 z / R} \left(\frac{1}{R} \frac{\partial u}{\partial \varphi} \right) + \frac{\partial v}{\partial x} \\
 \gamma_{xz} &= \frac{\partial u}{\partial z} + \frac{\partial w}{\partial x} \\
 \gamma_{\varphi z} &= \frac{1}{1 + \gamma_0 z / R} \left(\frac{1}{R} \frac{\partial w}{\partial \varphi} - \frac{v}{R} \right) + \frac{\partial v}{\partial z}
 \end{aligned}
 \tag{2}$$

By substituting Eq. (1), the expressions for displacement at any point within the shell, the linear strains in terms of middle surface displacements are obtained as follow:

$$\begin{aligned}
 \varepsilon_x &= \varepsilon_{x_0} + z\chi_x + z^2\varepsilon_{x_0}^* + z^3\chi_x^* \\
 \varepsilon_\varphi &= \frac{1}{1 + \gamma_0 z/R} (\varepsilon_{\varphi_0} + z\chi_\varphi + z^2\varepsilon_{\varphi_0}^* + z^3\chi_\varphi^*) \\
 \varepsilon_z &= \varepsilon_{z_0} + z\chi_z + z^2\varepsilon_{z_0}^* \\
 \gamma_{x\varphi} &= \frac{1}{1 + \gamma_0 z/R} (\varepsilon_{x\varphi_0} + z\chi_{x\varphi} + z^2\varepsilon_{x\varphi_0}^* + z^3\chi_{x\varphi}^*) + \\
 & (\varepsilon_{\varphi x_0} + z\chi_{\varphi x} + z^2\varepsilon_{\varphi x_0}^* + z^3\chi_{\varphi x}^*) \\
 \gamma_{xz} &= \beta_x + z\chi_{xz} + z^2\beta_x^* + z^3\chi_{xz}^* \\
 \gamma_{\varphi z} &= \frac{1}{1 + \gamma_0 z/R} (\beta_{\varphi_0} + z\chi_{\varphi z_0} + z^2\beta_{\varphi_0}^* + z^3\chi_{\varphi z_0}^*) + \\
 & (\beta_{\varphi_1} + z\chi_{\varphi z_1} + z^2\beta_{\varphi_1}^*)
 \end{aligned} \tag{3}$$

where:

$$\begin{aligned}
 \varepsilon_{x_0} &= \frac{\partial u_0}{\partial x}, \quad \chi_x = \frac{\partial \theta_x}{\partial x} \\
 \varepsilon_{x_0}^* &= \frac{\partial u_0^*}{\partial x}, \quad \chi_x^* = \frac{\partial \theta_x^*}{\partial x} \\
 \varepsilon_{\varphi_0} &= \frac{1}{R} \frac{\partial \nu_0}{\partial \varphi} + \frac{w_0}{R} \\
 \chi_\varphi &= \gamma_0 \frac{1}{R^2} \frac{\partial \nu_0}{\partial \varphi} + \frac{1}{R} \frac{\partial \theta_\varphi}{\partial \varphi} + \frac{\theta_z}{R} \\
 \varepsilon_{\varphi_0}^* &= \frac{1}{R} \frac{\partial \nu_0^*}{\partial \varphi} + \frac{w_0^*}{R}, \quad \chi_\varphi^* = \frac{1}{R} \frac{\partial \theta_\varphi^*}{\partial \varphi} + \frac{\theta_z^*}{R} \\
 \varepsilon_{z_0} &= \theta_z, \quad \chi_z = 2w_0^*, \quad \varepsilon_{z_0}^* = 3\theta_z^* \\
 \varepsilon_{x\varphi_0} &= \frac{\partial \nu_0}{\partial x}, \quad \chi_{x\varphi} = \gamma_0 \frac{1}{R} \frac{\partial \nu_0}{\partial x} + \frac{\partial \theta_\varphi}{\partial x}, \quad \varepsilon_{x\varphi_0}^* = \frac{\partial \nu_0^*}{\partial x}, \\
 \chi_{x\varphi}^* &= \frac{\partial \theta_\varphi^*}{\partial x}, \quad \varepsilon_{\varphi x_0} = \frac{1}{R} \frac{\partial u_0}{\partial \varphi}, \quad \chi_{\varphi x} = \frac{1}{R} \frac{\partial \theta_x}{\partial \varphi}, \\
 \varepsilon_{\varphi x_0}^* &= \frac{1}{R} \frac{\partial u_0^*}{\partial \varphi}, \quad \chi_{\varphi x}^* = \frac{1}{R} \frac{\partial \theta_x^*}{\partial \varphi} \\
 \beta_x &= \theta_x + \frac{\partial w_0}{\partial x}, \quad \chi_{xz} = 2u_0^* + \frac{\partial \theta_z}{\partial x} \\
 \beta_x^* &= 3\theta_x^* + \frac{\partial w_0^*}{\partial x}, \quad \chi_{xz}^* = \frac{\partial \theta_z^*}{\partial x} \\
 \beta_{\varphi_0} &= \frac{1}{R} \frac{\partial w_0}{\partial \varphi} - \frac{\nu_0}{R}, \quad \chi_{\varphi z_0} = \frac{1}{R} \frac{\partial \theta_z}{\partial \varphi} - \gamma_0 \frac{\nu_0}{R^2} - \frac{\theta_\varphi}{R},
 \end{aligned} \tag{4}$$

$$\begin{aligned}
 \beta_{\varphi_0}^* &= \frac{1}{R} \frac{\partial w_0^*}{\partial \varphi} - \frac{\nu_0^*}{R}, \quad \chi_{\varphi z_0}^* = \frac{1}{R} \frac{\partial \theta_z^*}{\partial \varphi} - \frac{1}{R} \frac{\theta_\varphi^*}{R} \\
 \beta_{\varphi_1} &= \gamma_0 \frac{\nu_0}{R} + \theta_\varphi, \quad \chi_{\varphi z_1} = 2\nu_0^*, \beta_{\varphi_1}^* = 3\theta_\varphi^*
 \end{aligned}$$

3. Stress- Strain Relations and Stress Resultants

For an orthotropic material, 3-D stress-strain relations are obtained by Hooke’s law as [1]:

$$\begin{Bmatrix} \sigma_1 \\ \sigma_2 \\ \sigma_3 \\ \tau_{12} \\ \tau_{13} \\ \tau_{23} \end{Bmatrix}^k = \begin{bmatrix} C_{11} & C_{12} & C_{13} & 0 & 0 & 0 \\ C_{12} & C_{22} & C_{23} & 0 & 0 & 0 \\ C_{13} & C_{23} & C_{33} & 0 & 0 & 0 \\ 0 & 0 & 0 & C_{44} & 0 & 0 \\ 0 & 0 & 0 & 0 & C_{55} & 0 \\ 0 & 0 & 0 & 0 & 0 & C_{66} \end{bmatrix}^K \begin{Bmatrix} \varepsilon_1 \\ \varepsilon_2 \\ \varepsilon_3 \\ \gamma_{12} \\ \gamma_{13} \\ \gamma_{23} \end{Bmatrix}^k \tag{5}$$

coefficients C_{ij} are defined as:

$$\begin{aligned}
 C_{11} &= \frac{E_{11}(1 - \nu_{23}\nu_{32})}{\nu^*}, \quad C_{12} = \frac{E_{11}(\nu_{21} + \nu_{31}\nu_{23})}{\nu^*} \\
 C_{13} &= \frac{E_{11}(\nu_{31} + \nu_{21}\nu_{32})}{\nu^*} \\
 C_{22} &= \frac{E_{22}(1 - \nu_{13}\nu_{31})}{\nu^*}, \quad C_{23} = \frac{E_{22}(\nu_{32} + \nu_{12}\nu_{31})}{\nu^*} \\
 C_{33} &= \frac{E_{33}(1 - \nu_{12}\nu_{21})}{\nu^*} \\
 C_{44} &= G_{12}, C_{55} = G_{13}, C_{66} = G_{23} \\
 \nu^* &= (1 - \nu_{12}\nu_{21} - \nu_{23}\nu_{32} - \nu_{13}\nu_{31} - 2\nu_{21}\nu_{32}\nu_{13})
 \end{aligned} \tag{6}$$

where E_{ij} are Young’s modulus of elasticity, ν_{ij} are Poisson’s ratio, G_{ij} are the shear moduli for composite material in different directions. The relation between off-axis stress and strain for the k^{th} layer of a multi-layered composite cylindrical shell is defined as follows:

$$\begin{Bmatrix} \sigma_x \\ \sigma_\phi \\ \sigma_z \\ \sigma_{x\phi} \\ \sigma_{xz} \\ \sigma_{\phi z} \end{Bmatrix}^k = \begin{bmatrix} Q_{11} & Q_{12} & Q_{13} & Q_{14} & 0 & 0 \\ Q_{12} & Q_{22} & Q_{23} & Q_{24} & 0 & 0 \\ Q_{13} & Q_{23} & Q_{33} & Q_{34} & 0 & 0 \\ Q_{14} & Q_{24} & Q_{34} & Q_{44} & 0 & 0 \\ 0 & 0 & 0 & 0 & Q_{55} & Q_{56} \\ 0 & 0 & 0 & 0 & Q_{56} & Q_{66} \end{bmatrix}^k \begin{Bmatrix} \varepsilon_x \\ \varepsilon_\phi \\ \varepsilon_z \\ \gamma_{x\phi} \\ \gamma_{xz} \\ \gamma_{\phi z} \end{Bmatrix}^k \tag{7}$$

where Q_{ij} are elements of the reduced stiffness matrix as defined in Appendix A.

By substituting Eq. (3) into Eq. (7) and integrating through the shell thickness, Eq. (7) is refined to:

$$\bar{\sigma} = D\bar{\varepsilon} \tag{8}$$

$$D = \begin{bmatrix} D_f & 0 \\ 0 & k_0 D_s \end{bmatrix}, D_f = \begin{bmatrix} D_m & D_{mc} \\ D_{bc} & D_b \end{bmatrix} \tag{9}$$

The matrices D_m, D_b, D_{mc}, D_{bc} and D_s are given in Appendix B. k_0 is the shear correction factor whose value is considered equal to 1 for higher-order theories and equal to $\pi^2/12$ first order shear deformation theory. In Appendix C, accurate method of calculation of integrals thorough the shell thickness in stress-resultant equations, including the $(1 + z/R)$ terms, are presented. $\bar{\varepsilon}$ and $\bar{\sigma}$, the middle surface strain vector and stress-resultant vector, respectively, in Eq. (8) are defined as follow:

$$\bar{\sigma} = \begin{pmatrix} N_x, N_\varphi, N_{\varphi x}, N_{x\varphi}, N_x^*, N_\varphi^*, N_{\varphi x}^*, N_{x\varphi}^*, N_z, \\ N_z^*, M_x, M_\varphi, M_{\varphi x}, M_{x\varphi}, M_x^*, M_\varphi^*, M_{\varphi x}^*, M_{x\varphi}^*, \\ M_z, Q_x, Q_\varphi, R_\varphi, Q_x^*, Q_\varphi^*, R_\varphi^*, S_x, S_\varphi, T_\varphi, S_x^*, S_\varphi^* \end{pmatrix}^T \tag{10}$$

$$\bar{\varepsilon} = \begin{pmatrix} \varepsilon_{x0}, \varepsilon_{\varphi0}, \varepsilon_{\varphi x0}, \varepsilon_{x\varphi0}, \varepsilon_{x0}^*, \varepsilon_{\varphi0}^*, \varepsilon_{\varphi x0}^*, \varepsilon_{x\varphi0}^*, \varepsilon_{z0}, \\ \varepsilon_{z0}^*, \chi_x, \chi_\varphi, \chi_{\varphi x}, \chi_{x\varphi}, \chi_x^*, \chi_\varphi^*, \chi_{\varphi x}^*, \chi_{x\varphi}^*, \chi_z, \beta_x, \\ \beta_{\varphi0}, \beta_{\varphi1}, \beta_x^*, \beta_{\varphi0}^*, \beta_{\varphi1}^*, \chi_{xz}, \chi_{\varphi z0}, \chi_{\varphi z1}, \chi_{xz}^*, \chi_{\varphi z0}^* \end{pmatrix}^T \tag{11}$$

The components of the stress-resultant vector $\bar{\sigma}$ for the composite shell are defined as:

$$\begin{bmatrix} N_x & M_x & N_x^* & M_x^* \\ N_{x\varphi} & M_{x\varphi} & N_{x\varphi}^* & M_{x\varphi}^* \\ Q_x & S_x & Q_x^* & S_x^* \\ R_\varphi & T_\varphi & R_\varphi^* & - \end{bmatrix} = \sum_{i=1}^{NL} \int_{z_i}^{z_{i+1}} \begin{Bmatrix} \sigma_x \\ \sigma_{x\varphi} \\ \sigma_{xz} \\ \tau_{\varphi z} \end{Bmatrix} \left(1, z, z^2, z^3\right) \left(1 + \frac{\gamma_0 z}{R}\right) dz \tag{12}$$

$$\begin{bmatrix} N_\varphi & M_\varphi & N_\varphi^* & M_\varphi^* \\ N_{\varphi x} & M_{\varphi x} & N_{\varphi x}^* & M_{\varphi x}^* \\ Q_\varphi & S_\varphi & Q_\varphi^* & S_\varphi^* \end{bmatrix} = \sum_{i=1}^{NL} \int_{z_i}^{z_{i+1}} \begin{Bmatrix} \sigma_\varphi \\ \sigma_{\varphi x} \\ \sigma_{\varphi z} \end{Bmatrix} \left(1, z, z^2, z^3\right) dz$$

$$\begin{bmatrix} N_z & M_z & N_z^* \end{bmatrix} = \sum_{i=1}^{NL} \int_{z_i}^{z_{i+1}} \sigma_z \left(1, z, z^2\right) \left(1 + \frac{\gamma_0 z}{R}\right) dz$$

where NL is the number of composite layers.

4. Governing Equations

Using Hamilton’s principle, the equations of motion for the free vibration analysis are obtained. It could be defined as follows in analytical form:

$$\delta \int_{t_1}^{t_2} [U - K - W] dt = 0 \tag{13}$$

where U is the total strain energy due to deformation, W is the potential of the external loads and K is the kinetic energy. Due to the assumption of the absence of damping and external loads, the Hamilton’s principle could be summarized as follows:

$$\delta \int_{t_1}^{t_2} [U - K] dt = 0 \tag{14}$$

U , the total strain energy due to deformation in Eq. (13) is defined as:

$$U = \frac{1}{2} \iiint_V \sigma_{ij} \varepsilon_{ij} dV \tag{15}$$

$$\int_0^t \delta U dt = \int_0^t \int_0^L \int_0^{2\pi} \int_{-h/2}^{h/2} \begin{bmatrix} \sigma_x \delta \varepsilon_x + \sigma_y \delta \varepsilon_y + \\ \sigma_z \delta \varepsilon_z + \sigma_{xy} \delta \gamma_{xy} + \\ \sigma_{xz} \delta \gamma_{xz} + \sigma_{yz} \delta \gamma_{yz} \end{bmatrix} dAdzdt$$

and the kinetic energy, K is defined as:

$$K = \frac{1}{2} \iiint_V \rho \left(\dot{u}^2 + \dot{v}^2 + \dot{w}^2 \right) dV \tag{16}$$

$$\int_0^t \delta K dt = - \int_0^t \int_0^L \int_0^{2\pi} \int_{-h/2}^{h/2} \rho (\ddot{u} \delta u + \ddot{v} \delta v + \ddot{w} \delta w) dAdzdt$$

ρ is the mass density of the material of the shell and $(\dot{})$ represents differentiation with respect to time. In Eqs. (15) and (16), the differential element on the middle surface of the shell is defined as [10]:

$$dA = R \left(1 + \frac{\gamma_0 z}{R}\right) dx d\varphi \tag{17}$$

Substituting the appropriate strain expressions given by Eq. (4) and the displacement expressions given by Eq. (1) in Eq. (14) and integrating the resulting expressions by parts, after separating the coefficients of $\delta u_0, \delta v_0, \delta w_0, \delta \theta_x, \delta \theta_\varphi, \delta \theta_z, \delta u_0^*, \delta v_0^*$,

δw_0^* , $\delta \theta_x^*$, $\delta \theta_\varphi^*$, $\delta \theta_z^*$, the equations of motions are obtained:

$$\begin{aligned} \delta u_0 : \\ \frac{\partial N_x}{\partial x} + \frac{1}{R} \frac{\partial N_{\varphi x}}{\partial \varphi} = \\ \frac{\partial^2 u_0}{\partial t^2} \bar{I}_0 + \frac{\partial^2 \theta_x}{\partial t^2} \bar{I}_1 + \frac{\partial^2 u_0^*}{\partial t^2} \bar{I}_2 + \frac{\partial^2 \theta_x^*}{\partial t^2} \bar{I}_3 \end{aligned} \quad (18a)$$

$$\begin{aligned} \delta v_0 : \\ \frac{1}{R} \frac{\partial N_\varphi}{\partial \varphi} + \gamma_0 \frac{1}{R^2} \frac{\partial M_\varphi}{\partial \varphi} + \frac{\partial N_{x\varphi}}{\partial x} + \gamma_0 \frac{1}{R} \frac{\partial M_{x\varphi}}{\partial x} + \\ \frac{1}{R} Q_\varphi - \gamma_0 \frac{1}{R} R_\varphi + \gamma_0 \frac{1}{R^2} S_\varphi = \\ \frac{\partial^2 v_0}{\partial t^2} \left(\bar{I}_0 + \frac{2\gamma_0}{R} \bar{I}_1 + \frac{\gamma_0}{R^2} \bar{I}_2 \right) + \frac{\partial^2 \theta_\varphi}{\partial t^2} \left(\bar{I}_1 + \frac{\gamma_0}{R} \bar{I}_2 \right) + \\ \frac{\partial^2 v_0^*}{\partial t^2} \left(\bar{I}_2 + \frac{\gamma_0}{R} \bar{I}_3 \right) + \frac{\partial^2 \theta_\varphi^*}{\partial t^2} \left(\bar{I}_3 + \frac{\gamma_0}{R} \bar{I}_4 \right) \end{aligned} \quad (18b)$$

$$\begin{aligned} \delta w_0 : \\ -\frac{1}{R} N_\varphi + \frac{\partial Q_x}{\partial x} + \frac{1}{R} \frac{\partial Q_\varphi}{\partial \varphi} = \\ \frac{\partial^2 w_0}{\partial t^2} \bar{I}_0 + \frac{\partial^2 \theta_z}{\partial t^2} \bar{I}_1 + \frac{\partial^2 w_0^*}{\partial t^2} \bar{I}_2 + \frac{\partial^2 \theta_z^*}{\partial t^2} \bar{I}_3 \end{aligned} \quad (18c)$$

$$\begin{aligned} \delta \theta_x : \\ \frac{\partial M_x}{\partial x} + \frac{1}{R} \frac{\partial M_{\varphi x}}{\partial \varphi} - Q_x = \\ \frac{\partial^2 u_0}{\partial t^2} \bar{I}_1 + \frac{\partial^2 \theta_x}{\partial t^2} \bar{I}_2 + \frac{\partial^2 u_0^*}{\partial t^2} \bar{I}_3 + \frac{\partial^2 \theta_x^*}{\partial t^2} \bar{I}_4 \end{aligned} \quad (18d)$$

$$\begin{aligned} \delta \theta_\varphi : \\ \frac{1}{R} \frac{\partial M_\varphi}{\partial \varphi} + \frac{\partial M_{x\varphi}}{\partial x} + \frac{1}{R} S_\varphi - R_\varphi = \\ \frac{\partial^2 v_0}{\partial t^2} \left(\bar{I}_1 + \frac{\gamma_0}{R} \bar{I}_2 \right) + \frac{\partial^2 \theta_\varphi}{\partial t^2} \bar{I}_2 + \frac{\partial^2 v_0^*}{\partial t^2} \bar{I}_3 + \frac{\partial^2 \theta_\varphi^*}{\partial t^2} \bar{I}_4 \end{aligned} \quad (18e)$$

$$\begin{aligned} \delta \theta_z : \\ -\frac{1}{R} M_\varphi - N_z + \frac{1}{R} \frac{\partial S_\varphi}{\partial \varphi} + \frac{\partial S_x}{\partial x} = \\ \frac{\partial^2 w_0}{\partial t^2} \bar{I}_1 + \frac{\partial^2 \theta_z}{\partial t^2} \bar{I}_2 + \frac{\partial^2 w_0^*}{\partial t^2} \bar{I}_3 + \frac{\partial^2 \theta_z^*}{\partial t^2} \bar{I}_4 \end{aligned} \quad (18f)$$

$$\begin{aligned} \delta u_0^* : \\ \frac{\partial N_x^*}{\partial x} + \frac{1}{R} \frac{\partial N_{\varphi x}^*}{\partial \varphi} - 2S_x = \end{aligned} \quad (18g)$$

$$\frac{\partial^2 u_0^*}{\partial t^2} \bar{I}_2 + \frac{\partial^2 \theta_x^*}{\partial t^2} \bar{I}_3 + \frac{\partial^2 u_0^*}{\partial t^2} \bar{I}_4 + \frac{\partial^2 \theta_x^*}{\partial t^2} \bar{I}_5$$

$$\begin{aligned} \delta v_0^* : \\ \frac{1}{R} \frac{\partial N_\varphi^*}{\partial \varphi} + \frac{\partial N_{x\varphi}^*}{\partial x} + \frac{1}{R} Q_\varphi^* - 2T_\varphi = \end{aligned} \quad (18h)$$

$$\frac{\partial^2 v_0^*}{\partial t^2} \left(\bar{I}_2 + \frac{\gamma_0}{R} \bar{I}_3 \right) + \frac{\partial^2 \theta_\varphi^*}{\partial t^2} \bar{I}_3 + \frac{\partial^2 v_0^*}{\partial t^2} \bar{I}_4 + \frac{\partial^2 \theta_\varphi^*}{\partial t^2} \bar{I}_5$$

$$\begin{aligned} \delta w_0^* : \\ -\frac{1}{R} N_\varphi^* - 2M_z + \frac{\partial Q_x^*}{\partial x} + \frac{1}{R} \frac{\partial Q_\varphi^*}{\partial \varphi} = \end{aligned} \quad (18i)$$

$$\frac{\partial^2 w_0^*}{\partial t^2} \bar{I}_2 + \frac{\partial^2 \theta_z^*}{\partial t^2} \bar{I}_3 + \frac{\partial^2 w_0^*}{\partial t^2} \bar{I}_4 + \frac{\partial^2 \theta_z^*}{\partial t^2} \bar{I}_5$$

$$\begin{aligned} \delta \theta_x^* : \\ \frac{\partial M_x^*}{\partial x} + \frac{1}{R} \frac{\partial M_{\varphi x}^*}{\partial \varphi} - 3Q_x^* = \end{aligned} \quad (18j)$$

$$\frac{\partial^2 u_0^*}{\partial t^2} \bar{I}_3 + \frac{\partial^2 \theta_x^*}{\partial t^2} \bar{I}_4 + \frac{\partial^2 u_0^*}{\partial t^2} \bar{I}_5 + \frac{\partial^2 \theta_x^*}{\partial t^2} \bar{I}_6$$

$$\begin{aligned} \delta \theta_\varphi^* : \\ \frac{1}{R} \frac{\partial M_\varphi^*}{\partial \varphi} + \frac{\partial M_{x\varphi}^*}{\partial x} + \frac{1}{R} S_\varphi^* - 3R_\varphi^* = \end{aligned} \quad (18k)$$

$$\frac{\partial^2 v_0^*}{\partial t^2} \left(\bar{I}_3 + \frac{\gamma_0}{R} \bar{I}_4 \right) + \frac{\partial^2 \theta_\varphi^*}{\partial t^2} \bar{I}_4 + \frac{\partial^2 v_0^*}{\partial t^2} \bar{I}_5 + \frac{\partial^2 \theta_\varphi^*}{\partial t^2} \bar{I}_6$$

$$\begin{aligned} \delta \theta_z^* : \\ -\frac{1}{R} M_\varphi^* - 3N_z^* + \frac{\partial S_x^*}{\partial x} + \frac{1}{R} \frac{\partial S_\varphi^*}{\partial \varphi} = \end{aligned} \quad (18l)$$

$$\frac{\partial^2 w_0^*}{\partial t^2} \bar{I}_3 + \frac{\partial^2 \theta_z^*}{\partial t^2} \bar{I}_4 + \frac{\partial^2 w_0^*}{\partial t^2} \bar{I}_5 + \frac{\partial^2 \theta_z^*}{\partial t^2} \bar{I}_6$$

where the inertia terms in the right side of Eqs. (18) are given by

$$\begin{aligned} (\bar{I}_0, \bar{I}_1, \bar{I}_2, \bar{I}_3, \bar{I}_4, \bar{I}_5, \bar{I}_6) = \\ \int_{\frac{h}{2}}^{\frac{h}{2}} \rho (1, z, z^2, z^3, z^4, z^5, z^6) (1 + \gamma_0 z / R) dz \end{aligned} \quad (19)$$

Natural and essential boundary conditions for simply supported conditions at $x=0$ and $x=L$ are as follows:

$$\begin{aligned}
 \delta u_0 = 0 \text{ or } N_x = 0, \quad \delta u_0^* = 0 \text{ or } N_x^* = 0, \\
 \delta v_0 = 0 \text{ or } (N_{x\varphi} + \gamma_0 / RM_{x\varphi}) = 0, \quad \delta v_0^* = 0 \\
 \text{or } N_{x\varphi}^* = 0, \\
 \delta w_0 = 0 \text{ or } Q_x = 0, \quad \delta w_0^* = 0 \text{ or } Q_x^* = 0, \\
 \delta \theta_x = 0 \text{ or } M_x = 0, \quad \delta \theta_x^* = 0 \text{ or } M_x^* = 0, \\
 \delta \theta_\varphi = 0 \text{ or } M_{x\varphi} = 0, \quad \delta \theta_\varphi^* = 0 \text{ or } M_{x\varphi}^* = 0, \\
 \delta \theta_z = 0 \text{ or } S_x = 0, \quad \delta \theta_z^* = 0 \text{ or } S_x^* = 0,
 \end{aligned} \tag{20}$$

5. Solution to the Governing Equations

The Galerkin method is used to solve the free vibration problem of simply supported-simply supported circular cylindrical composite shells. The boundary conditions for simply supported edges at $x=0$ and $x=L$ is applied as follows [10]:

$$\begin{aligned}
 v_0 = w_0 = \theta_\varphi = \theta_z = v_0^* = w_0^* = \\
 \theta_\varphi^* = \theta_z^* = N_x = M_x = N_x^* = M_x^* = 0
 \end{aligned} \tag{21}$$

In order to satisfy the boundary conditions, the displacement components are expanded as follow [6]:

$$\begin{aligned}
 u_0 &= u_{0mn}^* \cos \lambda x \cos n\varphi e^{i\omega_{mn}t} \\
 v_0 &= v_{0mn}^* \sin \lambda x \sin n\varphi e^{i\omega_{mn}t} \\
 w_0 &= w_{0mn}^* \sin \lambda x \cos n\varphi e^{i\omega_{mn}t} \\
 \theta_x &= \theta_{xmn}^* \cos \lambda x \cos n\varphi e^{i\omega_{mn}t} \\
 \theta_\varphi &= \theta_{\varphi mn}^* \sin \lambda x \sin n\varphi e^{i\omega_{mn}t} \\
 \theta_z &= \theta_{zmn}^* \sin \lambda x \cos n\varphi e^{i\omega_{mn}t} \\
 u_0^* &= u_{0mn}^* \cos \lambda x \cos n\varphi e^{i\omega_{mn}t} \\
 v_0^* &= v_{0mn}^* \sin \lambda x \sin n\varphi e^{i\omega_{mn}t} \\
 w_0^* &= w_{0mn}^* \sin \lambda x \cos n\varphi e^{i\omega_{mn}t} \\
 \theta_x^* &= \theta_{xmn}^* \cos \lambda x \cos n\varphi e^{i\omega_{mn}t} \\
 \theta_\varphi^* &= \theta_{\varphi mn}^* \sin \lambda x \sin n\varphi e^{i\omega_{mn}t} \\
 \theta_z^* &= \theta_{zmn}^* \sin \lambda x \cos n\varphi e^{i\omega_{mn}t}
 \end{aligned} \tag{22}$$

where in Eq. (22), $\lambda = m\pi/L$ and ω_{mn} are the natural angular frequencies (in rad/s) and are related to the mode numbers (m,n) where m is the axial half-wave number and n is the circumferential wave number.

$u_{0mn}^*, v_{0mn}^*, w_{0mn}^*, \theta_{xmn}^*, \theta_{\varphi mn}^*, \theta_{zmn}^*, u_{0mn}^*, v_{0mn}^*, w_{0mn}^*, \theta_{xmn}^*, \theta_{\varphi mn}^*, \theta_{zmn}^*$ are the constant amplitudes of vibrations related to the natural mode shapes. By substituting Eq. (22) into Eqs. (18) and applying the

Galerkin method, after simplification and collecting coefficients, the following eigenvalue equation is obtained:

$$[\mathbf{K} - \beta_{mn} \mathbf{M}]d = 0 \tag{23}$$

where is the displacement vector, d and $\beta_{mn} = \omega_{mn}^2$ corresponding to the mode shape numbers (m,n) . Generally, between the 12 eigenvalues (frequencies) obtained from Eq. (23), the smallest one is associated to the bending vibration mode shape corresponding to the specified mode numbers (m,n) . The lowest eigenvalue is called fundamental frequency of bending vibration. The elements of the stiffness matrix $[\mathbf{K}]$ and the mass matrix $[\mathbf{M}]$ are given in Appendix D.

6. Numerical Results and Discussion

In order to analyze the free vibration of composite circular cylindrical shells with simply supported-simply supported boundary conditions, a computer code using MATLABR13 based on the formulation of the present shell theories is developed. Different examples of composite cylindrical shells with a wide range of thickness-to-radius (h/R) and length-to-radius (L/R) ratios are investigated to show the efficiency and accuracy of the present formulations. In order to verify the present results, they were compared to the analytical results available in the literature. Furthermore, the results were validated with those obtained using Lanczos eigenfrequency extraction subroutine in ABAQUS/Standard code. In order to obtain accurate results of the free vibration analysis, the stress resultants were calculated using exact integration over the thickness of the composite cylindrical shells. In addition, in contrast to some 3-D elasticity theories, e.g. Refs. [1, 13], in the literature for the free vibration analysis, the present RHOST does not require any iterative procedure and convergence study. This is an advantage from the sense that computational time in the present RHOST is less than these iterative procedures.

Unless otherwise stated, the following geometrical and material properties are used hereinafter:

$$\begin{aligned}
 \frac{E_1}{E_1} = 40 \quad \frac{E_2}{E_3} = 1 \\
 \frac{G_{12}}{E_2} = \frac{G_{13}}{E_2} = 0.6 \quad \frac{G_{23}}{E_2} = 0.5 \\
 \nu_{12} = \nu_{13} = \nu_{23} = 0.25 \\
 Layup = [0/90], \frac{L}{R} = 1, \frac{h}{R} = 0.1
 \end{aligned} \tag{24}$$

Also, unless otherwise mentioned, the natural frequency parameter is considered to be:

$$\omega^* = \omega(h/\pi)\sqrt{\rho/G_{12}} \quad (25)$$

For the verification purpose, in Tables 1 to 4, the results of the present RHOST12 and HOST12 are compared to those obtained from 3-D elasticity exact solution method, reported by Ref. [13].

In Table 1, the lowest natural frequency parameters, ω^* , for 4-layered cylindrical shells having symmetric cross-ply layup are presented. As can be seen in this Table, in all cases, the first frequency parameters of $[0/90]_s$ layup are greater than those for $[90/0]_s$ layup. Furthermore, good accuracy is obtained in comparison with the results of Ref. [13] for different values of thickness ratios and mode shape numbers. By increasing h/R , the discrepancies are increased. Also, by increasing n , the discrepancies are increased for $[0/90]_s$ layup, unless at $n=3$ for $[90/0]_s$. The maximum discrepancy (1.75%) is corresponded to $h/R=0.3$ and $n=2$ for $[90/0]_s$ layup.

In Tables 2 and 3, the first three frequency parameters of cross-ply composite cylindrical shells are shown for different values of h/R , and circumferential mode number (n). The results were also validated by making comparison with Ref. [13]. According to these Tables, the natural frequency parameters of the laminated cylinders increased by increasing the number of layers. This trend occurs due to the fact that by increasing the number of layers, the bending-extensional coupling decreased for an anti-symmetric cross-ply laminate. It is necessary to be noted that in Tables 2 and 3, by increasing both h/R and n , the discrepancies increased. The maximum discrepancy for the present RHOST12 (2.84%) and for the present HOST12 (5.12%) are both corresponded to $h/R=0.3$ and $n=3$ for $[0/90]$

layup in Table 2. As shown in these Tables, all the discrepancies corresponding to the present RHOST12 are very less than those for the present HOST12. This outcome reveals the importance of incorporating the trapezoidal shape factor ($1+z/R$ terms) in the present analytical formulations. In addition, as can be seen in these Tables, except for $h/R=0.1$ for layup $[0/90]_2$ in Table 2, generally by increasing the number of layers, the discrepancies decreased. Also, good agreement between the present results of RHOST12 and Ref. [13] results shows the accuracy of the present theory.

Table 4 shows the values of the first three frequency parameters for different orthotropic ratios of 2-layered unsymmetric cross-ply composite cylindrical shells for different values of the thickness-to-radius ratio h/R . The present RHOST12 results were validated by making comparison with those reported by Ref. [13] and good agreement was observed. According to the results, all frequency parameters increased by increasing either the stiffness ratio E_1/E_2 or the thickness-to-radius ratio h/R of the cylinders. Also, the discrepancy increased by increasing the values of E_1/E_2 and h/R . The maximum discrepancy (5.6%) is corresponded to $E_1/E_2=40$ and $h/R=0.5$ for the second (II) frequency. There is not a specific trend for the discrepancies when the frequency number (I, II or III) is changed.

In Fig. 3, variations of the natural frequency parameter vs. thickness-to-radius (h/R) is indicated for symmetric cross-ply layups. Also, the results of the present RHOST12 and HOST12 theories for $L/R=10$ are compared with the present FEM analysis. According to Fig. 3(a) by decreasing the value of orthotropic ratio, E_1/E_2 , the discrepancies between the results of the present RHOST12 and HOST12 and the present FEM results increased specially for greater values of h/R .

Table 1. Natural frequency parameters, ω^* , for composite circular cylindrical shells with symmetric cross-ply layups ($m=1$)

h/R	Theory	$[0/90]_s$			$[90/0]_s$		
		$n=1$	$n=2$	$n=3$	$n=1$	$n=2$	$n=3$
0.1	RHOST12 (present)	0.079302	0.066377	0.064700	0.070809	0.052872	0.059267
	Ref. [13]	0.079277	0.066335	0.064600	0.070738	0.052748	0.059130
		0.03*	0.06	0.15	0.10	0.23	0.23
0.2	RHOST12 (present)	0.175333	0.163123	0.171778	0.151538	0.131548	0.160240
	Ref. [13]	0.175188	0.162844	0.170868	0.150651	0.130168	0.158886
		0.08	0.17	0.53	0.58	1.06	0.85
0.3	RHOST12 (present)	0.273215	0.263860	0.286369	0.239027	0.222623	0.272072
	Ref. [13]	0.272860	0.263048	0.283798	0.236385	0.218779	0.268258
		0.13	0.30	0.90	1.11	1.75	1.42

*Percentage discrepancy $((\text{Present} - \text{Ref. [13]}) / \text{Ref. [13]}) * 100$.

Table 2. Natural frequency parameters, ω^* , for composite circular cylindrical shells with unsymmetric cross-ply layups ($m=1$)

h/R	Theory	$[0 / 90]_1$						$[0 / 90]_2$					
		$n=1$		$n=2$		$n=3$		$n=1$		$n=2$		$n=3$	
0.1	RHOST12 (present)	0.069519	0.13*	0.049802	0.35	0.046207	0.56	0.074085	0.22	0.058276	0.52	0.059502	0.78
	HOST12 (present)	0.069594	0.24	0.049986	0.72	0.046627	1.46	0.074141	0.30	0.058461	0.84	0.059881	1.42
	Ref. [13]	0.069428		0.049630		0.045949		0.073919		0.057975		0.059043	
0.2	RHOST12 (present)	0.148051	0.84	0.122233	1.64	0.130875	1.99	0.162243	0.81	0.145715	1.48	0.162551	1.77
	HOST12 (present)	0.148539	1.17	0.123520	2.72	0.133160	3.77	0.162664	1.08	0.146790	2.23	0.164226	2.82
	Ref. [13]	0.146819		0.120255		0.128317		0.160932		0.143589		0.159729	
0.3	RHOST12 (present)	0.233711	1.61	0.208223	2.64	0.232943	2.84	0.253687	1.10	0.239751	1.82	0.272722	2.01
	HOST12 (present)	0.235187	2.24	0.211727	4.37	0.238106	5.12	0.254902	1.59	0.242367	2.94	0.276154	3.29
	Ref. [13]	0.230019		0.202861		0.226517		0.250922		0.235457		0.267347	

*Percentage discrepancy ((Present -Ref. [13])/ Ref. [13])*100.

Table 3. Natural frequency parameters, ω^* , for composite circular cylindrical shells with unsymmetric cross-ply layups ($m=1$)

h/R	Theory	$[0 / 90]_3$						$[0 / 90]_4$					
		$n=1$		$n=2$		$n=3$		$n=1$		$n=2$		$n=3$	
0.1	RHOST12 (present)	0.075019	0.11*	0.059930	0.24	0.062060	0.36	0.075390	0.07	0.060569	0.15	0.063045	0.24
	HOST12 (present)	0.075052	0.15	0.060071	0.48	0.062379	0.79	0.075408	0.09	0.060679	0.33	0.0632470	0.56
	Ref. [13]	0.074939		0.059787		0.061838		0.075339		0.060477		0.062896	
0.2	RHOST12 (present)	0.165499	0.39	0.151194	0.72	0.170352	0.90	0.166894	0.27	0.153521	0.49	0.173719	0.64
	HOST12 (present)	0.165812	0.58	0.152001	1.26	0.171439	1.55	0.167122	0.41	0.154138	0.89	0.174432	1.05
	Ref. [13]	0.164852		0.150114		0.168829		0.166445		0.152779		0.172616	
0.3	RHOST12 (present)	0.259425	0.57	0.249229	0.99	0.285798	1.20	0.262183	0.42	0.253746	0.75	0.292216	0.99
	HOST12 (present)	0.260390	0.95	0.251165	1.78	0.288778	1.93	0.262929	0.71	0.255779	1.32	0.293348	1.38
	Ref. [13]	0.257947		0.246783		0.282406		0.261081		0.251849		0.289353	

*Percentage discrepancy ((Present -Ref. [13])/ Ref. [13])*100.

Table 4. First three lowest frequency parameters, ω^* , for composite circular cylindrical shells with unsymmetric cross-ply layups ($m=n=1$)

$\frac{E_1}{E_2}$	Theory	$[0 / 90]$								
		$h/R=0.1$			$h/R=0.3$			$h/R=0.5$		
		I	II	III	I	II	III	I	II	III
10	RHOST12 (present)	0.06192	0.15824	0.29462	0.20945	0.47465	0.71821	0.38460	0.78261	0.98567
	Ref. [13]	0.06192	0.15824	0.29444	0.20878	0.47432	0.71297	0.38198	0.78053	0.96867
		0*	0	0.06	0.32	0.06	0.73	0.68	0.26	1.75
20	RHOST12 (present)	0.06632	0.20305	0.38953	0.22237	0.58876	0.80612	0.39948	0.92867	1.06172
	Ref. [13]	0.06629	0.20302	0.38888	0.22057	0.58695	0.79149	0.39425	0.91408	1.02944
		0.04	0.01	0.16	0.81	0.3	1.84	1.32	1.59	3.13
30	RHOST12 (present)	0.06828	0.23929	0.45417	0.22921	0.66924	0.85234	0.40660	1.00773	1.10908
	Ref. [13]	0.06823	0.23922	0.45285	0.22638	0.66463	0.82864	0.39975	0.97244	1.07140
		0.07	0.02	0.29	1.25	0.69	2.86	1.71	3.62	3.51
40	RHOST12 (present)	0.06951	0.27021	0.50185	0.23371	0.72855	0.88451	0.41091	1.05494	1.14304
	Ref. [13]	0.06943	0.27009	0.49971	0.23002	0.71976	0.85292	0.40298	0.99892	1.10068
		0.11	0.04	0.42	1.6	1.22	3.7	1.96	5.6	3.84

*Percentage discrepancy ((Present -Ref. [13])/ Ref. [13])*100.

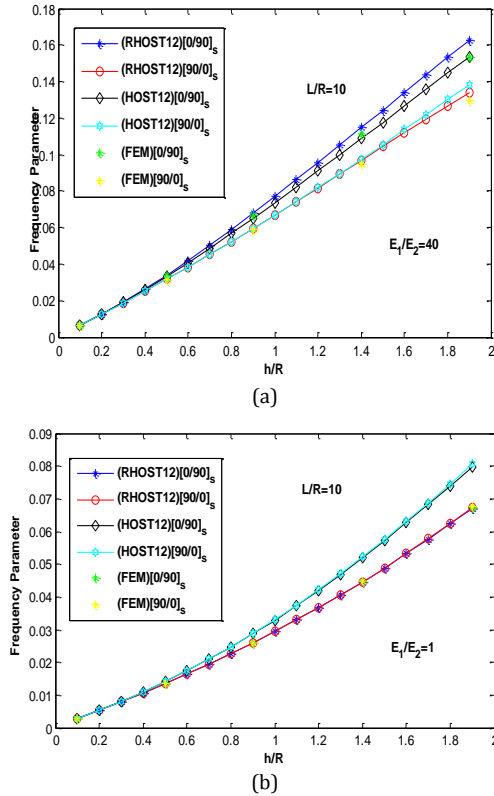


Fig. 3. Effect of layup on the lowest natural frequency parameter, ω^* , SS-SS composite cylinder vs. thickness-to-radius ratio (h/R); . (a). $E_1/E_2=40$ ($L/R=1$). (b). $E_1/E_2=1$ ($L/R=10$)

As illustrated in Fig. 3(a), at $h/R=1.9$, the discrepancies of the present RHOST12 and HOST12 for $E_1/E_2=40$ are 0.23% and 6.21% for $[0/90]_s$ layup and 3.19% and 6.66% for $[90/0]_s$ layup, respectively. At $h/R=1.9$, the discrepancies of the present RHOST12 and HOST12 for $E_1/E_2=1$ are -0.44% and 18.4% for $[0/90]_s$ layup and -0.43% and 19.33% for $[90/0]_s$ layup, respectively, as indicated in Fig. 3(b). Generally, the frequencies corresponded to $[0/90]_s$ layup are greater than $[90/0]_s$ layup.

In Figs. 4(a) and 4(b), variations of the lowest natural frequency parameter vs. L/R ratio is indicated for $[0/90]_s$ and $[0/90]_2$ layups of a cross-ply composite circular cylindrical shell for the present RHOST12 and HOST12. According to these figures, regardless of the layup sequence (symmetric or unsymmetric) for $h/R = 0.5$ and 1.5, by increasing L/R ratio from 5 to 20, the differences between the present RHOST12 and HOST12 increased from about 0% and 2% to about 2.63% and 6.7%, respectively.

Variations of the lowest natural frequency parameter, ω^* vs. h/R ratio, for different orthotropic ratios (E_1/E_2) are presented in Fig. 5. The results of the present HOST12 and RHOST12 are compared to each other for $L/R=1$ (Fig. 5(a)) and also to the present FEM results for $L/R=10$ (Fig. 5(b)).

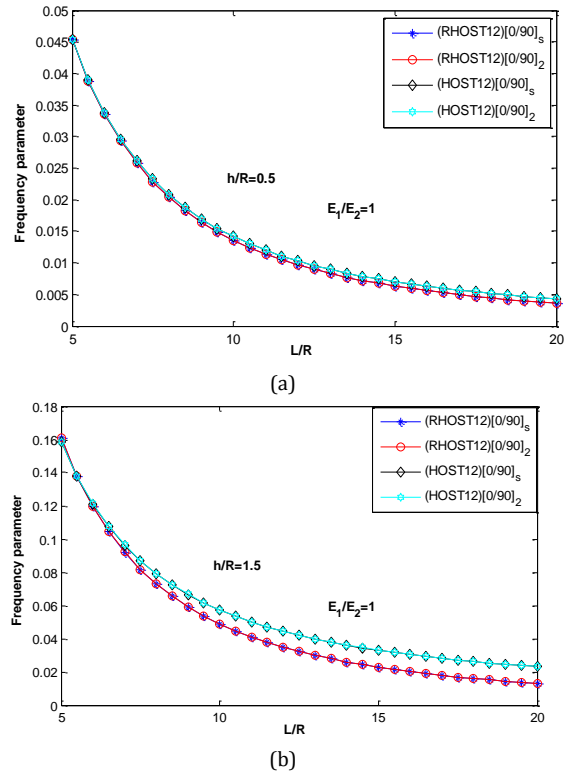


Fig. 4. Lowest natural frequency parameter, ω^* , SS-SS composite cylinder vs. length-to-radius ratio (L/R) for two different layups ; (a). $h/R=0.5$ ($E_1/E_2=1$). (b). $h/R=1.5$ ($E_1/E_2=1$).

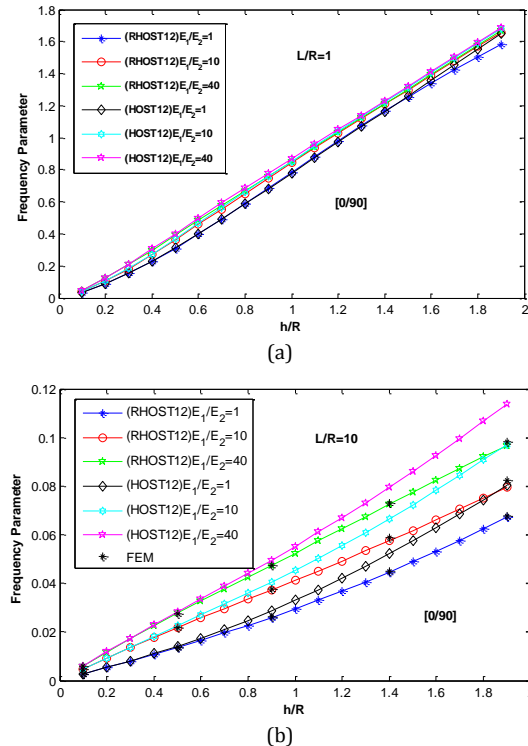


Fig. 5. Lowest natural frequency parameter ω^* , for SS-SS composite cylinder vs. thickness-to-radius ratio (h/R) for different orthotropic ratios (E_1/E_2); (a). $L/R=1$, (b). $L/R=10$.

As it can be seen in Fig. 5(a), regardless of the value of E_1/E_2 , the difference between the present RHOST12 and HOST12 results are not considerable since the shell length is short. However, according to Fig. 5. (b), by increasing h/R from 0.1 to 1.9, the discrepancies between the present RHOST12 and FEM for $E_1/E_2=1, 10$ and 40 increased from about 0% to about -0.67% -3.35% and -1.64%, and these discrepancies for HOST12 increased from about 0% to about 18.58%, 17.87% and 15.7%, respectively.

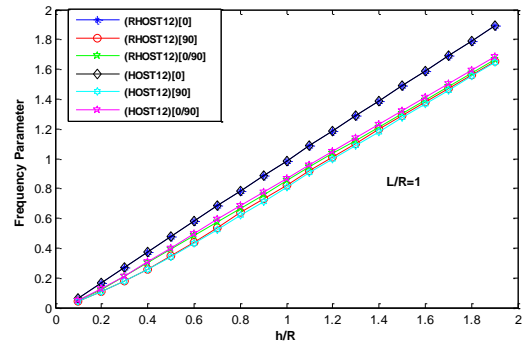
According to Fig. 5(b), there is a good agreement between the present RHOST12 and FEM results and noticeable discrepancies were found between HOST12 and FEM results.

Fig. 6(a) indicates the effect of different layups on the lowest natural frequency parameter vs. h/R ratio for $L/R=1$. In this figure, the maximum difference between the results of the present RHOST12 and HOST12 is about 1.01%. However, in the case of $L/R=10$, as indicated in Fig. 6(b), the geometric parameter L/R has considerable influence on the accuracy of the present theories. By increasing the value of L/R , the differences between the present HOST12 and RHOST12 increased. The results of the present FEM simulations are also compared. As it can be seen in Fig. 6(b), the maximum discrepancy -8.5% occurs in the case of [90] layup between the present HOST12 and FEM results.

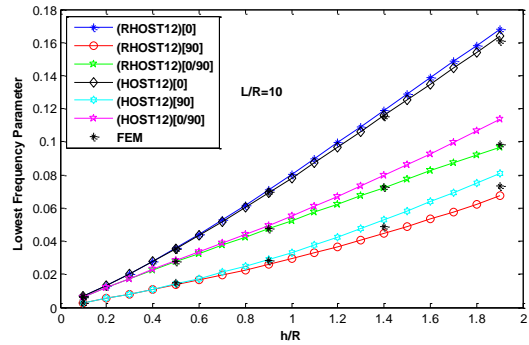
It could be observed from Figs. 6(a) and 6(b) that for both RHOST12 and HOST12 by increasing the volume fraction of zero angle layers in the laminate, the frequency of the cylinder increased.

Figs. 7(a) and 7(b) illustrate the variations of frequency parameter vs. orthotropic ratio E_1/E_2 for $L/R=1$ and 10 , respectively. In Fig. 7(a), a small difference between the present RHOST12 and HOST12 exists and it is almost unchanged by increasing the value of E_1/E_2 the present RHOST12 and HOST12. In addition, the frequency converges to an almost constant value. However, in case of $L/R=10$ in Fig. 7(b), by increasing E_1/E_2 and h/R , the differences between the present RHOST12 and HOST12 increased.

The maximum discrepancy (14.55%) between the present theories and the present FEM simulations occurs for HOST12 at $h/R=1.8$ and $E_1/E_2 =45$ as it can be seen in Fig. 7(b). In fact, by increasing the value of L/R , the influence of the exact integration of the stress resultants over the trapezoidal-like cross-section of the shell becomes more important. Since in the present HOST12, this important point is not considered, this theory fails to predict the correct values of the frequency in contrast to the present RHOST12 especially for higher values of h/R , E_1/E_2 and L/R ratios.

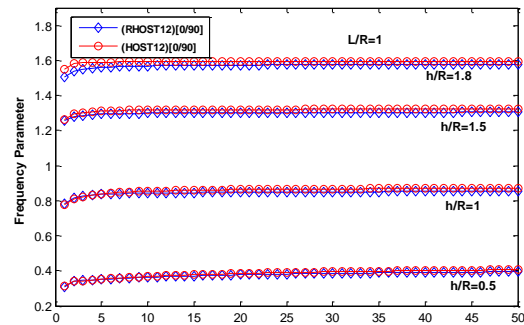


(a)

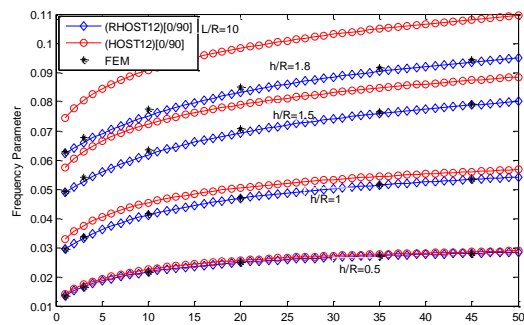


(b)

Fig. 6. Lowest natural frequency parameter ω^* , for SS-SS composite cylinder vs. thickness-to-radius ratio (h/R) for different cross-ply layups. (a). $L/R=1$. (b). $L/R=10$



(a)



(b)

Fig. 7. Lowest natural frequency parameter ω^* , for SS-SS composite cylinder vs. orthotropic ratio (E_1/E_2) for [0/90] layup. (a). $L/R=1$. (b). $L/R=10$.

In Fig. 8, variations of lowest natural frequency parameters, ω^* , vs. number of layers (n) in $[0/90]_n$ layup for different orthotropic ratios (E_1/E_2) have been investigated. As shown in Fig. 8(a), for $L/R=1$ and $h/R=0.1$, regardless of the value of E_1/E_2 , by increasing the number of layers (n) in $[0/90]_n$ layup, no considerable difference could be observed between the present RHOST12 and HOST12 results. Also, by increasing the number of layers in $[0/90]_n$ layup, regardless of the value of E_1/E_2 , the frequency converges to a special constant value. Furthermore, in Fig. 8(b), for $L/R=10$ and $h/R=1.5$, the frequency converges to another special constant value. However, in contrast to Fig. 8(a), considerable difference could be observed between the present RHOST12 and HOST12 results by changing the value of E_1/E_2 . For $E_1/E_2=1$, the differences between the present RHOST12 and HOST12 are almost unchanged by increasing the number of layers (n) in $[0/90]_n$ layup. While, for $E_1/E_2=10$ and 40 , there is a special value for the number of layers (n) where the difference between the present RHOST12 and HOST12 is negligible and before and after this special value, this difference becomes clear especially for lower values of the number of layers (n).

In Table 5, the lowest natural frequency parameters, ω^* , obtained from the present analytical theories are compared with those reported by Ref. [13]. In addition, results are compared to those obtained using Lanczos eigenvalue extraction method in ABAQUS/Standard solver and the associated mode shapes are depicted in Table 5. For the finite element 3-D (FE) modeling of the composite cylindrical shells, 8-noded continuum shell (SC8R) was used and convergence study for the elements size was achieved.

As it can be seen from Table 5, for the first bending mode No. (1,1), the absolute values of the discrepancies between the present theories and those of Ref. [13] for different thickness-to-radius ratios $h/R=0.1, 0.2$ and 0.3 are $0.13\%, 0.64\%$ and 1.61% , respectively, for RHOST12 and $0.24\%, 1.17\%$ and 2.24% , respectively, for HOST12. According to Table 5, for the second bending mode No. (1,2), the absolute values of discrepancies between the present theories and those of Ref. [13] for different thickness-to-radius ratios $h/R=0.1, 0.2$ and 0.3 are $0.35\%, 1.64\%$ and 2.64% , respectively, for RHOST12 and $0.72\%, 3.96\%$ and 7.44% , respectively, for HOST12.

Also, as shown in Table 5, for the third bending mode No. (1,3), the absolute values of the discrepancies between the present theories and those of

Ref. [13] for different thickness-to-radius ratios $h/R=0.1, 0.2$ and 0.3 are $0.56\%, 1.99\%$ and 2.84% , respectively, for RHOST12 and $1.41\%, 5.43\%$ and 8.87% , respectively, for HOST12. Hence, by increasing the mode number, generally the discrepancies increased for both the present RHOST12 and HOST12.

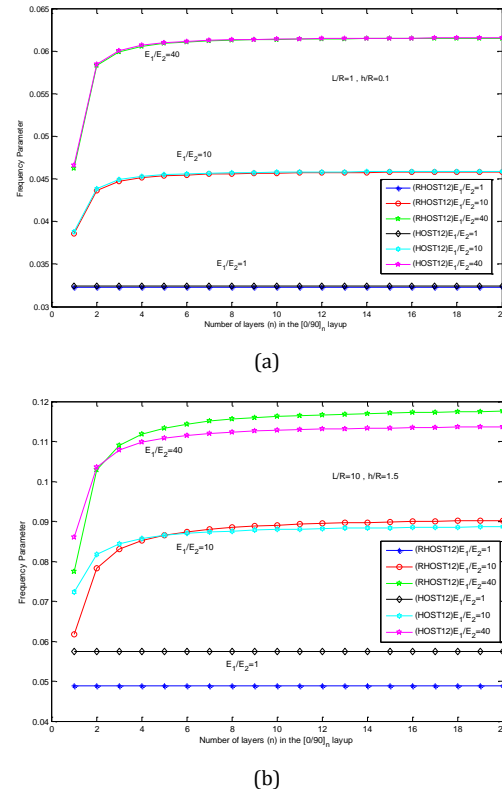
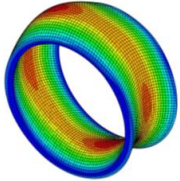
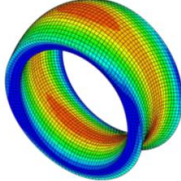
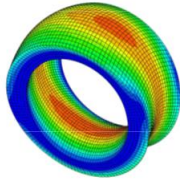
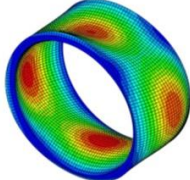
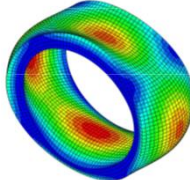
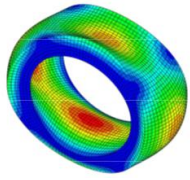
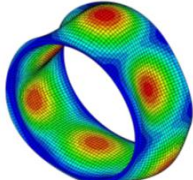
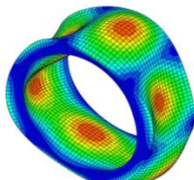
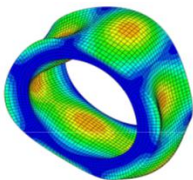


Fig. 8. Lowest natural frequency parameter ω^* , for SS-SS composite cylinder vs. number of layers (n) in $[0/90]_n$ layup for different orthotropic ratios (E_1/E_2). (a) $L/R=1$ and $h/R=0.1$. (b) $L/R=10$ and $h/R=1.5$

According to Table 5, the present FEM analysis also indicates good accuracy as compared to those results in Ref. [13]. For different thickness-to-radius ratios $h/R=0.1, 0.2$ and 0.3 , for the first mode (1,1), the discrepancies between the present FEM results and Ref. [13] are $0.04\%, 1.09\%$ and 0.69% , respectively. For the second bending mode (1,2), the discrepancies are $-0.02\%, -0.11\%$ and -1.43% , respectively, and for the third bending mode (1,3), the discrepancies are $-0.24\%, -1.78\%$ and -3.47% , respectively. As compared to Ref. [13], in most cases, the discrepancies of the present FEM results are less than those for the present RHOST12. However, in some cases like mode No. (1,1) with $h/R=0.2$ and mode no. (1,3) with $h/R=0.3$, the results of the present RHOST are closer than the present FEM results to those for Ref. [13].

Table 5. Comparison of lowest natural frequency parameters ω^* , for composite circular cylindrical shells with unsymmetric cross-ply layups [(0/90)] with those obtained using Lanczos method of eigenvalue extraction in ABAQUS/Standard solver and associated mode shapes (L/R=1).

Mode no. (m,n)	Theory	h/R=0.1		h/R=0.2		h/R=0.3	
(1,1)	Ref. [13]	0.069428		0.146819		0.230019	
	RHOST12 (present)	0.069519	0.13*	0.148051	0.84	0.233711	1.61
	HOST12 (present)	0.069594	0.24	0.148539	1.17	0.235178	2.24
	FEM (present)	0.069458	0.04	0.148423	1.09	0.231612	0.69
	FSDT(present)	0.069858	0.61	0.150135	2.25	0.239457	4.1
	<i>Mode shape</i>						
(1,2)	Ref. [13]	0.049630		0.120255		0.202861	
	RHOST12 (present)	0.049802	0.35	0.122233	1.64	0.208223	2.64
	HOST12 (present)	0.049986	0.72	0.123520	2.72	0.211727	4.37
	FEM (present)	0.049618	-0.02	0.120119	-0.11	0.199962	-1.43
	FSDT(present)	0.050340	1.43	0.125735	4.55	0.217378	7.15
	<i>Mode shape</i>						
(1,3)	Ref. [13]	0.045949		0.128317		0.226517	
	RHOST12 (present)	0.046207	0.56	0.130875	1.99	0.232943	2.84
	HOST12 (present)	0.046620	1.46	0.133160	3.77	0.238106	5.12
	FEM (present)	0.045838	-0.24	0.126032	-1.78	0.218653	-3.47
	FSDT(present)	0.047055	2.40	0.135579	5.65	0.244040	7.73
	<i>Mode shape</i>						

*Percentage discrepancy ((Present -Ref. [13])/ Ref. [13])*100.

7. Conclusions

For the first time, a closed form solution method for free vibration analysis of composite thin and thick simply supported cylindrical shells on the basis of 3-D refined higher-order shell theory (RHOST) is presented in this study. The effect of the trapezoidal shape factor (1+z/R terms) of the cross-section of the orthotropic composite circular cylindrical shells was incorporated exactly in the formulations. The characteristic eigenvalue equation was obtained based on Hamilton's principle and by applying Galerkin method to the governing equations, natural frequencies were obtained. The applicability and validity of the present theory were confirmed by verifying the results with those obtained using the

exact 3-D elasticity method for a wide range of thickness-to-radius and thickness-to-length ratios. Comparisons of the results for thick cylindrical shells with published results in the literature were carried out and good agreement was observed. The present theory does not require any convergence study, in contrast to some existing iterative approaches in the literature that require a few iterations to achieve sufficient convergence to the exact solution. This is an important advantage of the present RHOST. Furthermore, the natural frequencies associated to higher-modes of moderately thick, thick and very thick composite cylinders, never published in the literature before, were compared to those obtained using FE modeling in ABAQUS commercial software. The

results show that considering the effect of the $(1+z/R)$ terms in the calculation of stress resultants, would lead to a reliable higher-order theory for the

free vibration analysis of highly orthotropic composite circular cylindrical shells, especially for the cases of long and thick hollow cylinders.

Nomenclature

h	Shell's thickness
L	Length of the cylinder
R	Mean radius of the cylindrical shell
x	Position coordinate in axial direction
z	Position coordinate in radial direction
\emptyset	Position coordinate in tangential direction
u	Displacement component in axial direction
v	Displacement component in tangential direction
w	Displacement component in radial direction
γ_0	Coefficient of trapezoidal shape
$u_0, v_0, w_0, \theta_x, \theta_y, \theta_z, u_0^*, v_0^*, w_0^*, \theta_x^*, \theta_y^*, \theta_z^*$	Displacement component
$\varepsilon_x, \varepsilon_y, \varepsilon_z, \gamma_{xy}, \gamma_{xz}, \gamma_{yz}$	Strain components
$\bar{\varepsilon}$	Vector of strain components
$\bar{\sigma}$	Vector of stress resultants components
$\sigma_1, \sigma_2, \sigma_3, \tau_{12}, \tau_{13}, \tau_{23}$	Normal and shear stresses of each layer
$\varepsilon_1, \varepsilon_2, \varepsilon_3, \gamma_{12}, \gamma_{13}, \gamma_{23}$	Normal and shear strains of each layer
C_{ij}	Elements of stiffness matrix
Q_{ij}	Elements of reduced stiffness matrix
E_{11}, E_{22}, E_{33}	Young's modulus
G_{12}, G_{13}, G_{23}	Shear modulus
$\nu_{12}, \nu_{13}, \nu_{23}, \nu_{21}, \nu_{31}, \nu_{32}$	Poisson coefficients
θ	The rotation angle of the fiber relative to the main axis
$\sigma_x, \sigma_y, \sigma_z, \tau_{xy}, \tau_{xz}, \tau_{yz}$	Normal and shear stresses for a multilayer
NL	Number of layers
$D_f, D_m, D_{mc}, D_{bc}, D_b, D_s$	Shell stiffness matrices
U	Total strain energy
W	Energy from external forces
K	Total kinetic energy
$\bar{I}_0, \bar{I}_1, \bar{I}_2, \bar{I}_3, \bar{I}_4, \bar{I}_5, \bar{I}_6$	Shell mass inertia
L_{ij}	Differential operators
m	Number of half-axial waves
n	Number of circumferential waves
$T_{mn}(t)$	Time functions in generalized coordinates
ω_{mn}	Natural frequency for mode (m, n)
ω_f	Fundamental natural frequency
K	Stiffness matrix
$u_{0mn}, v_{0mn}, w_{0mn}, \theta_{xmn}, \theta_{ymn}, \theta_{zmn}, u_{0mn}^*, v_{0mn}^*, w_{0mn}^*, \theta_{xmn}^*, \theta_{ymn}^*, \theta_{zmn}^*$	Constant natural mode shapes

M	Mass matrix
k_0	Shear Correction Coefficient (first order shear deformation theory)
N_x, N_y, N_{xy}, N_{yx} ,	Stress resultants
$N_x^*, N_y^*, N_{xy}^*, N_{yx}^*, N_z, N_z^*$,	
M_x, M_y, M_{xy}, M_{yx} ,	Strain and curvature components
$M_x^*, M_y^*, M_{xy}^*, M_{yx}^*, M_z$,	
Q_x, R_x, Q_y, R_y ,	
$Q_x^*, R_x^*, Q_y^*, R_y^*$,	
$S_x, T_x, S_y, T_y, S_x^*, S_y^*$	
$\epsilon_{x_0}, \epsilon_{y_0}, \epsilon_{xy_0}, \epsilon_{yx_0}$,	
$\epsilon_{x_0}^*, \epsilon_{y_0}^*, \epsilon_{xy_0}^*, \epsilon_{yx_0}^*, \epsilon_{z_0}, \epsilon_{z_0}^*$,	
$\chi_x, \chi_y, \chi_{xy}, \chi_{yx}$,	
$\chi_x^*, \chi_y^*, \chi_{xy}^*, \chi_{yx}^*, \chi_z$,	
$\phi_{x_0}, \phi_{x_1}, \phi_{y_0}, \phi_{y_1}$,	
$\phi_{x_0}^*, \phi_{x_1}^*, \phi_{y_0}^*, \phi_{y_1}^*$,	
$\chi_{xz_0}, \chi_{xz_1}, \chi_{yz_0}, \chi_{yz_1}, \chi_{xz_0}^*, \chi_{yz_0}^*$	

Appendixes

Appendix A. Elements of Reduced Stiffness Matrix Q_{ij}

$$\begin{aligned}
 Q_{11} &= C_{11}c^4 + 2(C_{12} + 2C_{44})s^2c^2 + C_{22}s^4 \\
 Q_{12} &= C_{12}(c^4 + s^4) + (C_{11} + C_{22} - 2C_{44})s^2c^2 \\
 Q_{13} &= C_{13}c^2 + C_{23}s^2 \\
 Q_{14} &= (C_{11} - C_{12} - 2C_{44})sc^3 + (C_{12} - C_{22} + 2C_{44})cs^3 \\
 Q_{22} &= C_{11}s^4 + 2(C_{12} + 2C_{44})s^2c^2 + C_{22}c^4 \\
 Q_{23} &= C_{13}s^2 + C_{23}c^2 \\
 Q_{24} &= (C_{11} - C_{12} - 2C_{44})s^3c + (C_{12} - C_{22} + 2C_{44})c^3s \\
 Q_{33} &= C_{33} \\
 Q_{34} &= (C_{31} - C_{32})sc \\
 Q_{44} &= (C_{11} - 2C_{12} + C_{22} - 2C_{44})s^2c^2 + C_{44}(c^4 + s^4) \\
 Q_{55} &= C_{55}c^2 + C_{66}s^2 \\
 Q_{56} &= (C_{55} - C_{66})sc \\
 Q_{66} &= C_{55}s^2 + C_{66}c^2 \\
 Q_{ij} &= Q_{ji} \quad , \quad i, j = 1, \dots, 6
 \end{aligned}$$

where $c = \cos \theta$ and $s = \sin \theta$; θ is fibre orientation (in radians) with respect to x-axis of the shell.

Appendix B. Definition of D matrices

The terms H_j , \bar{H}_j and \hat{H}_j ($j=1, 2, \dots, 7$), used in the following matrices (D_m, D_{mc}, D_{bc}, D_b , and D_s), are defined in Appendix C.

$$D_{m \ 10 \times 10} = \sum_{k=1}^{NL} \begin{bmatrix} Q_{11} \hat{H}_1 & Q_{12} H_1 & Q_{14} H_1 & Q_{14} \hat{H}_1 & Q_{11} \hat{H}_3 & Q_{12} H_3 & Q_{14} H_3 & Q_{14} \hat{H}_3 & Q_{13} \hat{H}_1 & Q_{13} \hat{H}_3 \\ Q_{12} H_1 & Q_{22} \bar{H}_1 & Q_{24} \bar{H}_1 & Q_{24} H_1 & Q_{12} H_3 & Q_{22} \bar{H}_3 & Q_{24} \bar{H}_3 & Q_{24} H_3 & Q_{23} H_1 & Q_{23} H_3 \\ Q_{14} H_1 & Q_{24} \bar{H}_1 & Q_{44} \bar{H}_1 & Q_{44} H_1 & Q_{14} H_3 & Q_{24} \bar{H}_3 & Q_{44} \bar{H}_3 & Q_{44} H_3 & Q_{34} H_1 & Q_{34} H_3 \\ Q_{14} \hat{H}_1 & Q_{24} H_1 & Q_{44} H_1 & Q_{44} \hat{H}_1 & Q_{14} \hat{H}_3 & Q_{24} H_3 & Q_{44} H_3 & Q_{44} \hat{H}_3 & Q_{34} \hat{H}_1 & Q_{34} \hat{H}_3 \\ Q_{11} \hat{H}_3 & Q_{12} H_3 & Q_{14} H_3 & Q_{14} \hat{H}_3 & Q_{11} \hat{H}_5 & Q_{12} H_5 & Q_{14} H_5 & Q_{14} \hat{H}_5 & Q_{13} \hat{H}_3 & Q_{13} \hat{H}_5 \\ Q_{12} H_3 & Q_{22} \bar{H}_3 & Q_{24} \bar{H}_3 & Q_{24} H_3 & Q_{12} H_5 & Q_{22} \bar{H}_5 & Q_{24} \bar{H}_5 & Q_{24} H_5 & Q_{23} H_3 & Q_{23} H_5 \\ Q_{14} H_3 & Q_{24} \bar{H}_3 & Q_{44} \bar{H}_3 & Q_{44} H_3 & Q_{14} H_5 & Q_{24} \bar{H}_5 & Q_{44} \bar{H}_5 & Q_{44} H_5 & Q_{34} H_3 & Q_{34} H_5 \\ Q_{14} \hat{H}_3 & Q_{24} H_3 & Q_{44} H_3 & Q_{44} \hat{H}_3 & Q_{14} \hat{H}_5 & Q_{24} H_5 & Q_{44} H_5 & Q_{44} \hat{H}_5 & Q_{34} \hat{H}_3 & Q_{34} \hat{H}_5 \\ Q_{13} \hat{H}_1 & Q_{23} \hat{H}_1 & Q_{34} \hat{H}_1 & Q_{34} \hat{H}_1 & Q_{13} \hat{H}_3 & Q_{23} \hat{H}_3 & Q_{34} \hat{H}_3 & Q_{34} \hat{H}_3 & Q_{33} \hat{H}_1 & Q_{33} \hat{H}_3 \\ Q_{13} \hat{H}_3 & Q_{23} \hat{H}_3 & Q_{34} \hat{H}_3 & Q_{34} \hat{H}_3 & Q_{13} \hat{H}_5 & Q_{23} \hat{H}_5 & Q_{34} \hat{H}_5 & Q_{34} \hat{H}_5 & Q_{33} \hat{H}_3 & Q_{33} \hat{H}_5 \end{bmatrix}^k$$

$$D_{mc \ 10 \times 9} = \sum_{k=1}^{NL} \begin{bmatrix} Q_{11} \hat{H}_2 & Q_{12} H_2 & Q_{14} H_2 & Q_{14} \hat{H}_2 & Q_{11} \hat{H}_4 & Q_{12} H_4 & Q_{14} H_4 & Q_{14} \hat{H}_4 & Q_{13} \hat{H}_2 & Q_{13} \hat{H}_4 \\ Q_{12} H_2 & Q_{22} \bar{H}_2 & Q_{24} \bar{H}_2 & Q_{24} H_2 & Q_{12} H_4 & Q_{22} \bar{H}_4 & Q_{24} \bar{H}_4 & Q_{24} H_4 & Q_{23} H_2 & Q_{23} H_4 \\ Q_{14} H_2 & Q_{24} \bar{H}_2 & Q_{44} \bar{H}_2 & Q_{44} H_2 & Q_{14} H_4 & Q_{24} \bar{H}_4 & Q_{44} \bar{H}_4 & Q_{44} H_4 & Q_{34} H_2 & Q_{34} H_4 \\ Q_{14} \hat{H}_2 & Q_{24} H_2 & Q_{44} H_2 & Q_{44} \hat{H}_2 & Q_{14} \hat{H}_4 & Q_{24} H_4 & Q_{44} H_4 & Q_{44} \hat{H}_4 & Q_{34} \hat{H}_2 & Q_{34} \hat{H}_4 \\ Q_{11} \hat{H}_4 & Q_{12} H_4 & Q_{14} H_4 & Q_{14} \hat{H}_4 & Q_{11} \hat{H}_6 & Q_{12} H_6 & Q_{14} H_6 & Q_{14} \hat{H}_6 & Q_{13} \hat{H}_4 & Q_{13} \hat{H}_6 \\ Q_{12} H_4 & Q_{22} \bar{H}_4 & Q_{24} \bar{H}_4 & Q_{24} H_4 & Q_{12} H_6 & Q_{22} \bar{H}_6 & Q_{24} \bar{H}_6 & Q_{24} H_6 & Q_{23} H_4 & Q_{23} H_6 \\ Q_{14} H_4 & Q_{24} \bar{H}_4 & Q_{44} \bar{H}_4 & Q_{44} H_4 & Q_{14} H_6 & Q_{24} \bar{H}_6 & Q_{44} \bar{H}_6 & Q_{44} H_6 & Q_{34} H_4 & Q_{34} H_6 \\ Q_{14} \hat{H}_4 & Q_{24} H_4 & Q_{44} H_4 & Q_{44} \hat{H}_4 & Q_{14} \hat{H}_6 & Q_{24} H_6 & Q_{44} H_6 & Q_{44} \hat{H}_6 & Q_{34} \hat{H}_4 & Q_{34} \hat{H}_6 \\ Q_{13} \hat{H}_2 & Q_{23} \hat{H}_2 & Q_{34} \hat{H}_2 & Q_{34} \hat{H}_2 & Q_{13} \hat{H}_4 & Q_{23} \hat{H}_4 & Q_{34} \hat{H}_4 & Q_{34} \hat{H}_4 & Q_{33} \hat{H}_2 & Q_{33} \hat{H}_4 \\ Q_{13} \hat{H}_4 & Q_{23} \hat{H}_4 & Q_{34} \hat{H}_4 & Q_{34} \hat{H}_4 & Q_{13} \hat{H}_6 & Q_{23} \hat{H}_6 & Q_{34} \hat{H}_6 & Q_{34} \hat{H}_6 & Q_{33} \hat{H}_4 & Q_{33} \hat{H}_6 \end{bmatrix}^k$$

$$D_{bc \ 9 \times 10} = \sum_{k=1}^{NL} \begin{bmatrix} Q_{11} \hat{H}_2 & Q_{12} H_2 & Q_{14} H_2 & Q_{14} \hat{H}_2 & Q_{11} \hat{H}_4 & Q_{12} H_4 & Q_{14} H_4 & Q_{14} \hat{H}_4 & Q_{13} \hat{H}_2 & Q_{13} \hat{H}_4 \\ Q_{12} H_2 & Q_{22} \bar{H}_2 & Q_{24} \bar{H}_2 & Q_{24} H_2 & Q_{12} H_4 & Q_{22} \bar{H}_4 & Q_{24} \bar{H}_4 & Q_{24} H_4 & Q_{23} H_2 & Q_{23} H_4 \\ Q_{14} H_2 & Q_{24} \bar{H}_2 & Q_{44} \bar{H}_2 & Q_{44} H_2 & Q_{14} H_4 & Q_{24} \bar{H}_4 & Q_{44} \bar{H}_4 & Q_{44} H_4 & Q_{34} H_2 & Q_{34} H_4 \\ Q_{14} \hat{H}_2 & Q_{24} H_2 & Q_{44} H_2 & Q_{44} \hat{H}_2 & Q_{14} \hat{H}_4 & Q_{24} H_4 & Q_{44} H_4 & Q_{44} \hat{H}_4 & Q_{34} \hat{H}_2 & Q_{34} \hat{H}_4 \\ Q_{11} \hat{H}_4 & Q_{12} H_4 & Q_{14} H_4 & Q_{14} \hat{H}_4 & Q_{11} \hat{H}_6 & Q_{12} H_6 & Q_{14} H_6 & Q_{14} \hat{H}_6 & Q_{13} \hat{H}_4 & Q_{13} \hat{H}_6 \\ Q_{12} H_4 & Q_{22} \bar{H}_4 & Q_{24} \bar{H}_4 & Q_{24} H_4 & Q_{12} H_6 & Q_{22} \bar{H}_6 & Q_{24} \bar{H}_6 & Q_{24} H_6 & Q_{23} H_4 & Q_{23} H_6 \\ Q_{14} H_4 & Q_{24} \bar{H}_4 & Q_{44} \bar{H}_4 & Q_{44} H_4 & Q_{14} H_6 & Q_{24} \bar{H}_6 & Q_{44} \bar{H}_6 & Q_{44} H_6 & Q_{34} H_4 & Q_{34} H_6 \\ Q_{14} \hat{H}_4 & Q_{24} H_4 & Q_{44} H_4 & Q_{44} \hat{H}_4 & Q_{14} \hat{H}_6 & Q_{24} H_6 & Q_{44} H_6 & Q_{44} \hat{H}_6 & Q_{34} \hat{H}_4 & Q_{34} \hat{H}_6 \\ Q_{13} \hat{H}_2 & Q_{23} \hat{H}_2 & Q_{34} \hat{H}_2 & Q_{34} \hat{H}_2 & Q_{13} \hat{H}_4 & Q_{23} \hat{H}_4 & Q_{34} \hat{H}_4 & Q_{34} \hat{H}_4 & Q_{33} \hat{H}_2 & Q_{33} \hat{H}_4 \end{bmatrix}^k$$

$$D_{b_{9 \times 9}} = \sum_{k=1}^{NL} \begin{bmatrix} Q_{11} \hat{H}_3 & Q_{12} H_3 & Q_{14} \hat{H}_3 & Q_{14} \hat{H}_3 & Q_{11} \hat{H}_5 & Q_{12} H_5 & Q_{14} H_5 & Q_{14} \hat{H}_5 & Q_{13} \hat{H}_3 \\ Q_{12} H_3 & Q_{22} \bar{H}_3 & Q_{24} \bar{H}_3 & Q_{24} H_3 & Q_{12} H_5 & Q_{22} \bar{H}_5 & Q_{24} \bar{H}_5 & Q_{24} H_5 & Q_{23} H_3 \\ Q_{14} H_3 & Q_{24} \bar{H}_3 & Q_{44} \bar{H}_3 & Q_{44} H_3 & Q_{14} H_5 & Q_{24} \bar{H}_5 & Q_{44} \bar{H}_5 & Q_{44} H_5 & Q_{34} H_3 \\ Q_{14} \hat{H}_3 & Q_{24} H_3 & Q_{44} H_3 & Q_{44} \hat{H}_3 & Q_{14} \hat{H}_5 & Q_{24} H_5 & Q_{44} H_5 & Q_{44} \hat{H}_5 & Q_{34} \hat{H}_3 \\ Q_{11} \hat{H}_5 & Q_{12} H_5 & Q_{14} \hat{H}_5 & Q_{14} \hat{H}_5 & Q_{11} \hat{H}_7 & Q_{12} H_7 & Q_{14} H_7 & Q_{14} \hat{H}_7 & Q_{13} \hat{H}_5 \\ Q_{12} H_5 & Q_{22} \bar{H}_5 & Q_{24} \bar{H}_5 & Q_{24} H_5 & Q_{12} H_7 & Q_{22} \bar{H}_7 & Q_{24} \bar{H}_7 & Q_{24} H_7 & Q_{23} H_5 \\ Q_{14} H_5 & Q_{24} \bar{H}_5 & Q_{44} \bar{H}_5 & Q_{44} H_5 & Q_{14} H_7 & Q_{24} \bar{H}_7 & Q_{44} \bar{H}_7 & Q_{44} H_7 & Q_{34} H_5 \\ Q_{14} \hat{H}_5 & Q_{24} H_5 & Q_{44} H_5 & Q_{44} \hat{H}_5 & Q_{14} \hat{H}_7 & Q_{24} H_7 & Q_{44} H_7 & Q_{44} \hat{H}_7 & Q_{34} \hat{H}_5 \\ Q_{13} \hat{H}_3 & Q_{23} \hat{H}_3 & Q_{34} \hat{H}_3 & Q_{34} \hat{H}_3 & Q_{13} \hat{H}_5 & Q_{23} \hat{H}_5 & Q_{34} \hat{H}_5 & Q_{34} \hat{H}_5 & Q_{33} \hat{H}_3 \end{bmatrix}^k$$

$$D_{s_{11 \times 11}} = \sum_{k=1}^{NL} \begin{bmatrix} Q_{55} \hat{H}_1 & Q_{56} H_1 & Q_{56} \hat{H}_1 & Q_{55} \hat{H}_3 & Q_{56} H_3 & Q_{56} \hat{H}_3 & Q_{55} \hat{H}_2 & Q_{56} H_2 & Q_{56} \hat{H}_2 & Q_{55} \hat{H}_4 & Q_{56} H_4 \\ & Q_{66} \bar{H}_1 & Q_{66} H_1 & Q_{56} H_3 & Q_{66} \bar{H}_3 & Q_{66} H_3 & Q_{56} H_2 & Q_{66} \bar{H}_2 & Q_{66} H_2 & Q_{56} H_4 & Q_{66} \bar{H}_4 \\ & & Q_{66} \hat{H}_1 & Q_{56} \hat{H}_3 & Q_{66} H_3 & Q_{66} \hat{H}_3 & Q_{56} \hat{H}_2 & Q_{66} H_2 & Q_{66} \hat{H}_2 & Q_{56} \hat{H}_4 & Q_{66} H_4 \\ & & & Q_{55} \hat{H}_5 & Q_{56} H_5 & Q_{56} \hat{H}_5 & Q_{55} \hat{H}_4 & Q_{56} H_4 & Q_{56} \hat{H}_4 & Q_{55} \hat{H}_6 & Q_{56} H_6 \\ & & & & Q_{66} \bar{H}_5 & Q_{66} H_5 & Q_{56} H_4 & Q_{66} \bar{H}_4 & Q_{66} H_4 & Q_{56} H_6 & Q_{66} \bar{H}_6 \\ & & & & & Q_{66} \hat{H}_5 & Q_{56} \hat{H}_4 & Q_{66} \hat{H}_4 & Q_{66} \hat{H}_4 & Q_{56} \hat{H}_6 & Q_{66} H_6 \\ & & & & & & Q_{55} \hat{H}_3 & Q_{56} H_3 & Q_{56} \hat{H}_3 & Q_{55} \hat{H}_5 & Q_{56} H_5 \\ & & & & & & & Q_{66} \bar{H}_3 & Q_{66} H_3 & Q_{56} H_5 & Q_{66} \bar{H}_5 \\ & & & & & & & & Q_{66} \hat{H}_3 & Q_{56} \hat{H}_5 & Q_{66} H_5 \\ & & & & & & & & & Q_{55} \hat{H}_7 & Q_{56} H_7 \\ & & & & & & & & & & Q_{66} \bar{H}_7 \end{bmatrix}^k$$

Sym.

Appendix C. Definition of H Components

In matrices $D_m, D_{mc}, D_{bc}, D_b,$ and D_s the terms H_j, \bar{H}_j and \hat{H}_j are defined as follows:

C.1. Definition of H_j

$$H_{j+1} = \frac{(z_{k+1}^{j+1} - z_k^{j+1})}{j+1}, \quad H_j = \frac{(z_{k+1}^j - z_k^j)}{j} \tag{C-1}$$

C.2. Definition of \hat{H}_j

$$\hat{H}_j = \int_{h_k}^{h_{k+1}} z^{j-1} (1 + \gamma_0 z / R) dz = H_j + \gamma_0 \frac{1}{R} H_{j+1}, \quad j = 1, 2, \dots, 7 \tag{C-2}$$

where H_j are defined in Eq. (C-1)

C.3. Definition of \bar{H}_j

$$\bar{H}_j = \int_{h_k}^{h_{k+1}} \frac{z^{j-1}}{1 + \gamma_0 z / R} dz \tag{C-3}$$

In the case of $\gamma_0 = 0$:

$$\bar{H}_j = H_j \tag{C-4}$$

In the case of $\gamma_0 = 1$ after taking exact integration through the thickness of each layer, the following results were obtained:

$$\begin{aligned}
 \bar{H}_1 &= \int_{h_k}^{h_{k+1}} \frac{1}{1+z/R} dz = R \left[\ln \left(\frac{R+h_{k+1}}{R+h_k} \right) \right] \\
 \bar{H}_2 &= \int_{h_k}^{h_{k+1}} \frac{z}{1+z/R} dz = R \left[(h_{k+1} - h_k) - R \ln \left(\frac{R+h_{k+1}}{R+h_k} \right) \right] \\
 \bar{H}_3 &= \int_{h_k}^{h_{k+1}} \frac{z^2}{1+z/R} dz = R \left[\frac{1}{2} (h_{k+1}^2 - h_k^2) - R(h_{k+1} - h_k) + R^2 \ln \left(\frac{R+h_{k+1}}{R+h_k} \right) \right] \\
 \bar{H}_4 &= \int_{h_k}^{h_{k+1}} \frac{z^3}{1+z/R} dz = R \left[\frac{1}{3} (h_{k+1}^3 - h_k^3) - \frac{1}{2} R(h_{k+1}^2 - h_k^2) + R^2(h_{k+1} - h_k) - R^3 \ln \left(\frac{R+h_{k+1}}{R+h_k} \right) \right] \\
 \bar{H}_5 &= \int_{h_k}^{h_{k+1}} \frac{z^4}{1+z/R} dz = R \left[\frac{1}{4} (h_{k+1}^4 - h_k^4) - \frac{1}{3} R(h_{k+1}^3 - h_k^3) + \frac{1}{2} R^2(h_{k+1}^2 - h_k^2) - R^3(h_{k+1} - h_k) + R^4 \ln \left(\frac{R+h_{k+1}}{R+h_k} \right) \right] \\
 \bar{H}_6 &= \int_{h_k}^{h_{k+1}} \frac{z^5}{1+z/R} dz = R \left[\frac{1}{5} (h_{k+1}^5 - h_k^5) - \frac{1}{4} R(h_{k+1}^4 - h_k^4) + \frac{1}{3} R^2(h_{k+1}^3 - h_k^3) - \frac{1}{2} R^3(h_{k+1}^2 - h_k^2) + \right. \\
 &\quad \left. R^4(h_{k+1} - h_k) - R^5 \ln \left(\frac{R+h_{k+1}}{R+h_k} \right) \right] \\
 \bar{H}_7 &= \int_{h_k}^{h_{k+1}} \frac{z^6}{1+z/R} dz = R \left[\frac{1}{6} (h_{k+1}^6 - h_k^6) - \frac{1}{5} R(h_{k+1}^5 - h_k^5) + \frac{1}{4} R^2(h_{k+1}^4 - h_k^4) - \frac{1}{3} R^3(h_{k+1}^3 - h_k^3) \right. \\
 &\quad \left. + \frac{1}{2} R^4(h_{k+1}^2 - h_k^2) - R^5(h_{k+1} - h_k) + R^6 \ln \left(\frac{R+h_{k+1}}{R+h_k} \right) \right]
 \end{aligned} \tag{C-5}$$

Appendix D. Elements of Stiffness and Mass Matrices

D.1. Elements of Stiffness Matrix $K_{12 \times 12}$:

$$\begin{aligned}
 K_{11} &= (D_{m11})(-\lambda^2) + \left(\frac{1}{R^2} D_{m33}\right)(-n^2), \quad K_{12} = \left(\frac{1}{R} D_{m12} + \frac{1}{R} D_{m34}\right)(\lambda n), \quad K_{13} = \left(\frac{1}{R} D_{m12}\right)(\lambda), \\
 K_{14} &= (D_{mc11})(-\lambda^2) + \left(\frac{1}{R^2} D_{mc33}\right)(-n^2), \quad K_{16} = (D_{m19})(\lambda), \quad K_{17} = (D_{m15})(-\lambda^2) + \left(\frac{1}{R^2} D_{m37}\right)(-n^2), \\
 K_{18} &= \left(\frac{1}{R} D_{m16} + \frac{1}{R} D_{m38}\right)(\lambda n), \quad K_{19} = \left(\frac{1}{R} D_{m16} + 2D_{mc19}\right)(\lambda), \quad K_{110} = (D_{mc15})(-\lambda^2) + \left(\frac{1}{R^2} D_{mc37}\right)(-n^2), \\
 K_{112} &= (3D_{m110})(\lambda), \quad K_{21} = \left(\frac{1}{R} D_{m21} + \frac{1}{R} D_{m43}\right)(\lambda n), \\
 K_{22} &= (D_{m44} + \frac{\gamma_0}{R} D_{mc44} + \frac{\gamma_0}{R} D_{bc44} + \frac{\gamma_0}{R^2} D_{b44})(-\lambda^2) + \left(\frac{1}{R^2} D_{m22} + \frac{\gamma_0}{R^3} D_{mc22} + \frac{\gamma_0}{R^3} D_{bc22} \right. \\
 &\quad \left. + \frac{\gamma_0}{R^4} D_{b22}\right)(-n^2) + \left(-\frac{1}{R^2} D_{s22} + \frac{\gamma_0}{R^2} D_{s23} - \frac{\gamma_0}{R^3} D_{s28} - \frac{\gamma_0}{R^3} D_{s82} - \frac{\gamma_0}{R^4} D_{s88} + \frac{\gamma_0}{R^2} D_{s32} - \frac{\gamma_0}{R^2} D_{s33}\right) \\
 K_{23} &= \left(\frac{1}{R^2} D_{m22} + \frac{1}{R^2} D_{s22} + \frac{\gamma_0}{R^3} D_{bc22} + \frac{\gamma_0}{R^3} D_{s82} - \frac{\gamma_0}{R^2} D_{s32}\right)(-n), \quad K_{24} = \left(\frac{\gamma_0}{R^2} D_{b21} + \frac{\gamma_0}{R^2} D_{b43}\right)(\lambda n),
 \end{aligned}$$

$$\begin{aligned}
 K_{25} &= (D_{mc44} + \frac{\gamma_0}{R} D_{b44})(-\lambda^2) + (\frac{1}{R^2} D_{mc22} + \frac{\gamma_0}{R^3} D_{b22})(-n^2) \\
 &\quad + (\frac{1}{R} D_{s23} - \frac{1}{R^2} D_{s28} - \frac{\gamma_0}{R^3} D_{s88} - \frac{\gamma_0}{R} D_{s33}) \\
 K_{26} &= (\frac{1}{R} D_{m29} + \frac{1}{R^2} D_{mc22} + \frac{1}{R^2} D_{s28} + \frac{\gamma_0}{R^3} D_{b22} + \frac{\gamma_0}{R^3} D_{s88})(-n), \quad K_{27} = (\frac{1}{R} D_{m25} + \frac{1}{R} D_{m47})(\lambda n), \\
 K_{28} &= (D_{m48} + \frac{\gamma_0}{R} D_{bc48})(-\lambda^2) + (\frac{1}{R^2} D_{m26} + \frac{\gamma_0}{R^3} D_{bc26})(-n^2) \\
 &\quad + (-\frac{1}{R^2} D_{s25} - \frac{\gamma_0}{R^3} D_{s85} + 2\frac{\gamma_0}{R^2} D_{s89} + \frac{\gamma_0}{R^2} D_{s35} - 2\frac{\gamma_0}{R} D_{s39}) \\
 K_{29} &= (\frac{1}{R^2} D_{m26} + \frac{1}{R^2} D_{s25} + \frac{\gamma_0}{R^3} D_{bc26} + 2\frac{\gamma_0}{R^2} D_{b29} + \frac{\gamma_0}{R^3} D_{s85} - \frac{\gamma_0}{R^2} D_{s35})(-n), \quad K_{210} = (\frac{\gamma_0}{R^2} D_{b25} + \frac{\gamma_0}{R^2} D_{b47})(\lambda n), \\
 K_{211} &= (D_{mc48} + \frac{\gamma_0}{R} D_{b48})(-\lambda^2) + (\frac{1}{R^2} D_{mc26} + \frac{\gamma_0}{R^3} D_{b26})(-n^2) + (\frac{3}{R} D_{s26} - \frac{1}{R^2} D_{s211} \\
 &\quad - \frac{\gamma_0}{R^3} D_{s811} - 3\frac{\gamma_0}{R} D_{s36}) \\
 K_{212} &= (\frac{3}{R} D_{m210} + \frac{1}{R^2} D_{mc26} + \frac{1}{R^2} D_{s211} + \frac{\gamma_0}{R^3} D_{b26} + \frac{\gamma_0}{R^3} D_{s811})(-n), \quad K_{31} = (-\frac{1}{R} D_{m21})(-\lambda), \\
 K_{32} &= (-\frac{1}{R^2} D_{m22} - \frac{\gamma_0}{R^3} D_{mc22} - \frac{1}{R^2} D_{s22} + \frac{\gamma_0}{R^2} D_{s23} - \frac{\gamma_0}{R^3} D_{s28})(n), \\
 K_{33} &= (D_{s11})(-\lambda^2) + (\frac{1}{R^2} D_{s22})(-n^2) + (-\frac{1}{R^2} D_{m22}), \quad K_{34} = (+D_{s11})(-\lambda), \quad K_{35} = (-\frac{1}{R^2} D_{mc22} + \frac{1}{R} D_{s23} - \frac{1}{R^2} D_{s28})(n), \\
 K_{36} &= (D_{s17})(-\lambda^2) + (\frac{1}{R^2} D_{s28})(-n^2) + (-\frac{1}{R} D_{m29} - \frac{1}{R^2} D_{mc22}), \quad K_{37} = (-\frac{1}{R} D_{m25} + 2D_{s17})(-\lambda), \\
 K_{38} &= (-\frac{1}{R^2} D_{m26} - \frac{1}{R^2} D_{s25})(n), \quad K_{39} = (D_{s14})(-\lambda^2) + (\frac{1}{R^2} D_{s25})(-n^2) + (-\frac{1}{R^2} D_{m26}), \quad K_{310} = (3D_{s14})(-\lambda), \\
 K_{311} &= (-\frac{1}{R^2} D_{mc26} + \frac{3}{R} D_{s26} - \frac{1}{R^2} D_{s211})(n), \quad K_{312} = (D_{s110})(-\lambda^2) + (\frac{1}{R^2} D_{s211})(-n^2) + (-\frac{3}{R} D_{m210} - \frac{1}{R^2} D_{mc26}), \\
 K_{41} &= (D_{bc11})(-\lambda^2) + (\frac{1}{R^2} D_{bc33})(-n^2), \quad K_{42} = (\frac{\gamma_0}{R^2} D_{b12} + \frac{\gamma_0}{R^2} D_{b34})(\lambda n), \quad K_{43} = (-D_{s11})(\lambda), \\
 K_{44} &= (D_{b11})(-\lambda^2) + (\frac{1}{R^2} D_{b33})(-n^2) + (-D_{s11}), \quad K_{45} = (\frac{1}{R} D_{b12} + \frac{1}{R} D_{b34})(\lambda n), \quad K_{46} = (D_{bc19} + \frac{1}{R} D_{b12} - D_{s17})(\lambda), \\
 K_{47} &= (D_{bc15})(-\lambda^2) + (\frac{1}{R^2} D_{bc37})(-n^2) + (-2D_{s17}), \quad K_{49} = (2D_{b19} - D_{s14})(\lambda), \\
 K_{410} &= (D_{b15})(-\lambda^2) + (\frac{1}{R^2} D_{b37})(-n^2) + (-3D_{s14}), \quad K_{411} = (\frac{1}{R} D_{b16} + \frac{1}{R} D_{b38})(\lambda n), \\
 K_{412} &= (3D_{bc110} + \frac{1}{R} D_{b16} - D_{s110})(\lambda), \\
 K_{52} &= (D_{bc44} + \frac{\gamma_0}{R} D_{b44})(-\lambda^2) + (\frac{1}{R^2} D_{bc22} + \frac{\gamma_0}{R^3} D_{b22})(-n^2) + (-\frac{1}{R^2} D_{s82} - \frac{\gamma_0}{R^3} D_{s88} \\
 &\quad + \frac{1}{R} D_{s32} - \frac{\gamma_0}{R} D_{s33}) \\
 K_{53} &= (\frac{1}{R^2} D_{bc22} + \frac{1}{R^2} D_{s82} - \frac{1}{R} D_{s32})(-n), \quad K_{54} = (\frac{1}{R} D_{b21} + \frac{1}{R} D_{b43})(\lambda n),
 \end{aligned}$$

$$\begin{aligned}
K_{55} &= (D_{b44})(-\lambda^2) + \left(\frac{1}{R^2} D_{b22}\right)(-n^2) + \left(-\frac{1}{R^2} D_{s88} - D_{s33}\right), K_{56} = \left(\frac{1}{R^2} D_{b22} + \frac{1}{R^2} D_{s88}\right)(-n), \\
K_{58} &= (D_{bc48})(-\lambda^2) + \left(\frac{1}{R^2} D_{bc26}\right)(-n^2) + \left(-\frac{1}{R^2} D_{s85} + \frac{2}{R} D_{s89} + \frac{1}{R} D_{s35} - 2D_{s39}\right), \\
K_{59} &= \left(\frac{1}{R^2} D_{bc26} + \frac{2}{R} D_{b29} + \frac{1}{R^2} D_{s85} - \frac{1}{R} D_{s35}\right)(-n), K_{510} = \left(\frac{1}{R} D_{b25} + \frac{1}{R} D_{b47}\right)(\lambda n), \\
K_{511} &= (D_{b48})(-\lambda^2) + \left(\frac{1}{R^2} D_{b26}\right)(-n^2) + \left(-\frac{1}{R^2} D_{s811} - 3D_{s36}\right), K_{512} = \left(\frac{1}{R^2} D_{b26} + \frac{1}{R^2} D_{s811}\right)(-n), K_{61} = (-D_{m91})(-\lambda), \\
K_{62} &= \left(-\frac{1}{R^2} D_{bc22} - \frac{\gamma_0}{R^3} D_{b22} - \frac{1}{R} D_{m92} - \frac{\gamma_0}{R^2} D_{mc92} - \frac{1}{R^2} D_{s82} - \frac{\gamma_0}{R^3} D_{s88}\right)(n), \\
K_{63} &= (D_{s71})(-\lambda^2) + \left(\frac{1}{R^2} D_{s82}\right)(-n^2) + \left(-\frac{1}{R^2} D_{bc22} - \frac{1}{R} D_{m92}\right), K_{64} = \left(-\frac{1}{R} D_{b21} - D_{mc91} + D_{s71}\right)(-\lambda), \\
K_{65} &= \left(-\frac{1}{R^2} D_{b22} - \frac{1}{R} D_{mc92} - \frac{1}{R^2} D_{s88}\right)(n), K_{66} = (D_{s77})(-\lambda^2) + \left(\frac{1}{R^2} D_{s88}\right)(-n^2) + \left(-\frac{1}{R^2} D_{b22} - D_{m99} - \frac{1}{R} D_{mc92}\right), \\
K_{67} &= (-D_{m95} + 2D_{s77})(-\lambda), K_{68} = \left(-\frac{1}{R^2} D_{bc26} - \frac{1}{R} D_{m96} - \frac{1}{R^2} D_{s85} + \frac{2}{R} D_{s89}\right)(n), \\
K_{69} &= (D_{s74})(-\lambda^2) + \left(\frac{1}{R^2} D_{s85}\right)(-n^2) + \left(-\frac{1}{R^2} D_{bc26} - \frac{2}{R} D_{b29} - \frac{1}{R} D_{m96} - 2D_{mc99}\right), \\
K_{610} &= \left(-\frac{1}{R} D_{b25} - D_{mc95} + 3D_{s74}\right)(-\lambda), K_{611} = \left(-\frac{1}{R^2} D_{b26} - \frac{1}{R} D_{mc96} - \frac{1}{R^2} D_{s811}\right)(n) \\
K_{612} &= (D_{s710})(-\lambda^2) + \left(\frac{1}{R^2} D_{s811}\right)(-n^2) + \left(-\frac{1}{R^2} D_{b26} - 3D_{m910} - \frac{1}{R} D_{mc96}\right), K_{71} = (D_{m51})(-\lambda^2) + \left(\frac{1}{R^2} D_{m73}\right)(-n^2), \\
K_{72} &= \left(\frac{1}{R} D_{m52} + \frac{1}{R} D_{m74}\right)(\lambda n), K_{73} = \left(\frac{1}{R} D_{m52} - 2D_{s71}\right)(\lambda), K_{74} = (D_{mc51})(-\lambda^2) + \left(\frac{1}{R^2} D_{mc73}\right)(-n^2) + (-2D_{s71}), \\
K_{76} &= (D_{m59} - 2D_{s77})(\lambda), K_{77} = (D_{m55})(-\lambda^2) + \left(\frac{1}{R^2} D_{m77}\right)(-n^2) + (-4D_{s77}), K_{78} = \left(\frac{1}{R} D_{m56} + \frac{1}{R} D_{m78}\right)(\lambda n), \\
K_{79} &= \left(\frac{1}{R} D_{m56} + 2D_{mc59} - 2D_{s74}\right)(\lambda), K_{710} = (D_{mc55})(-\lambda^2) + \left(\frac{1}{R^2} D_{mc77}\right)(-n^2) + (-6D_{s74}), \\
K_{712} &= (3D_{m510} - 2D_{s710})(\lambda), K_{81} = \left(\frac{1}{R} D_{m61} + \frac{1}{R} D_{m83}\right)(\lambda n), \\
K_{82} &= (D_{m84} + \frac{\gamma_0}{R} D_{mc84})(-\lambda^2) + \left(\frac{1}{R^2} D_{m62} + \frac{\gamma_0}{R^3} D_{mc62}\right)(-n^2) + \left(-\frac{1}{R^2} D_{s52} + \frac{\gamma_0}{R^2} D_{s53} - \frac{\gamma_0}{R^3} D_{s58} \right. \\
&\quad \left. - 2\frac{\gamma_0}{R} D_{s93} + 2\frac{\gamma_0}{R^2} D_{s98}\right), \\
K_{83} &= \left(\frac{1}{R^2} D_{m62} + \frac{1}{R^2} D_{s52}\right)(-n), K_{85} = (D_{mc84})(-\lambda^2) + \left(\frac{1}{R^2} D_{mc62}\right)(-n^2) + \left(\frac{1}{R} D_{s53} - \frac{1}{R^2} D_{s58} - 2D_{s93} + \frac{2}{R} D_{s98}\right), \\
K_{86} &= \left(\frac{1}{R} D_{m69} + \frac{1}{R^2} D_{mc62} + \frac{1}{R^2} D_{s58} - \frac{2}{R} D_{s98}\right)(-n), K_{87} = \left(\frac{1}{R} D_{m65} + \frac{1}{R} D_{m87}\right)(\lambda n), \\
K_{88} &= (D_{m88})(-\lambda^2) + \left(\frac{1}{R^2} D_{m66}\right)(-n^2) + \left(-\frac{1}{R^2} D_{s55} - 4D_{s99}\right), K_{89} = \left(\frac{1}{R^2} D_{m66} + \frac{1}{R^2} D_{s55}\right)(-n), \\
K_{811} &= (D_{mc88})(-\lambda^2) + \left(\frac{1}{R^2} D_{mc66}\right)(-n^2) + \left(\frac{3}{R} D_{s56} - \frac{1}{R^2} D_{s511} - 6D_{s96} + \frac{2}{R} D_{s911}\right), \\
K_{812} &= \left(\frac{3}{R} D_{m610} + \frac{1}{R^2} D_{mc66} + \frac{1}{R^2} D_{s511} - \frac{2}{R} D_{s911}\right)(-n), K_{91} = \left(-\frac{1}{R} D_{m61} - 2D_{bc91}\right)(-\lambda),
\end{aligned}$$

$$\begin{aligned}
 K_{92} &= \left(-\frac{1}{R^2} D_{m62} - \frac{\gamma_0}{R^3} D_{mc62} - \frac{2}{R} D_{bc92} - 2\frac{\gamma_0}{R^2} D_{b92} - \frac{1}{R^2} D_{s52} + \frac{\gamma_0}{R^2} D_{s53} - \frac{\gamma_0}{R^3} D_{s58}\right)(n), \\
 K_{93} &= (D_{s41})(-\lambda^2) + \left(\frac{1}{R^2} D_{s52}\right)(-n^2) + \left(-\frac{1}{R^2} D_{m62} - \frac{2}{R} D_{bc92}\right), K_{94} = (-2D_{b91} + D_{s41})(-\lambda), \\
 K_{95} &= \left(-\frac{1}{R^2} D_{mc62} - \frac{2}{R} D_{b92} + \frac{1}{R} D_{s53} - \frac{1}{R^2} D_{s58}\right)(n), \\
 K_{96} &= (D_{s47})(-\lambda^2) + \left(\frac{1}{R^2} D_{s58}\right)(-n^2) + \left(-\frac{1}{R} D_{m69} - \frac{1}{R^2} D_{mc62} - 2D_{bc99} - \frac{2}{R} D_{b92}\right), \\
 K_{97} &= \left(-\frac{1}{R} D_{m65} - 2D_{bc95} + 2D_{s47}\right)(-\lambda), K_{98} = \left(-\frac{1}{R^2} D_{m66} - \frac{2}{R} D_{bc96} - \frac{1}{R^2} D_{s55}\right)(n) \\
 K_{99} &= (D_{s44})(-\lambda^2) + \left(\frac{1}{R^2} D_{s55}\right)(-n^2) + \left(-\frac{1}{R^2} D_{m66} - \frac{2}{R} D_{bc96} - 4D_{b99}\right), K_{910} = (-2D_{b95} + 3D_{s44})(-\lambda), \\
 K_{911} &= \left(-\frac{1}{R^2} D_{mc66} - \frac{2}{R} D_{b96} + \frac{3}{R} D_{s56} - \frac{1}{R^2} D_{s511}\right)(n), \\
 K_{912} &= (D_{s410})(-\lambda^2) + \left(\frac{1}{R^2} D_{s511}\right)(-n^2) + \left(-\frac{3}{R} D_{m610} - \frac{1}{R^2} D_{mc66} - 6D_{bc910} - \frac{2}{R} D_{b96}\right), \\
 K_{101} &= (D_{bc51})(-\lambda^2) + \left(\frac{1}{R^2} D_{bc73}\right)(-n^2), K_{102} = \left(\frac{\gamma_0}{R^2} D_{b52} + \frac{\gamma_0}{R^2} D_{b74}\right)(\lambda n), K_{103} = (-3D_{s41})(\lambda), \\
 K_{104} &= (D_{b51})(-\lambda^2) + \left(\frac{1}{R^2} D_{b73}\right)(-n^2) + (-3D_{s41}), K_{105} = \left(\frac{1}{R} D_{b52} + \frac{1}{R} D_{b74}\right)(\lambda n), \\
 K_{106} &= (D_{bc59} + \frac{1}{R} D_{b52} - 3D_{s47})(\lambda), K_{107} = (D_{bc55})(-\lambda^2) + \left(\frac{1}{R^2} D_{bc77}\right)(-n^2) + (-6D_{s47}), K_{109} = (2D_{b59} - 3D_{s44})(\lambda), \\
 K_{1010} &= (D_{b55})(-\lambda^2) + \left(\frac{1}{R^2} D_{b77}\right)(-n^2) + (-9D_{s44}), K_{1011} = \left(\frac{1}{R} D_{b56} + \frac{1}{R} D_{b78}\right)(\lambda n), \\
 K_{1012} &= (3D_{bc510} + \frac{1}{R} D_{b56} - 3D_{s410})(\lambda), \\
 K_{112} &= (D_{bc84} + \frac{\gamma_0}{R} D_{b84})(-\lambda^2) + \left(\frac{1}{R^2} D_{bc62} + \frac{\gamma_0}{R^3} D_{b62}\right)(-n^2) + \left(-\frac{1}{R^2} D_{s112} - \frac{\gamma_0}{R^3} D_{s118}\right. \\
 &\quad \left.+ \frac{3}{R} D_{s62} - 3\frac{\gamma_0}{R} D_{s63}\right), \\
 K_{113} &= \left(\frac{1}{R^2} D_{bc62} + \frac{1}{R^2} D_{s112} - \frac{3}{R} D_{s62}\right)(-n), K_{114} = \left(\frac{1}{R} D_{b61} + \frac{1}{R} D_{b83}\right)(\lambda n), \\
 K_{115} &= (D_{b84})(-\lambda^2) + \left(\frac{1}{R^2} D_{b62}\right)(-n^2) + \left(-\frac{1}{R^2} D_{s118} - 3D_{s63}\right), \\
 K_{118} &= (D_{bc88})(-\lambda^2) + \left(\frac{1}{R^2} D_{bc66}\right)(-n^2) + \left(-\frac{1}{R^2} D_{s115} + \frac{2}{R} D_{s119} + \frac{3}{R} D_{s65} - 6D_{s69}\right), \\
 K_{119} &= \left(\frac{1}{R^2} D_{bc66} + \frac{2}{R} D_{b69} + \frac{1}{R^2} D_{s115} - \frac{3}{R} D_{s65}\right)(-n), K_{1110} = \left(\frac{1}{R} D_{b65} + \frac{1}{R} D_{b87}\right)(\lambda n), \\
 K_{1111} &= (D_{b88})(-\lambda^2) + \left(\frac{1}{R^2} D_{b66}\right)(-n^2) + \left(-\frac{1}{R^2} D_{s1111} - 9D_{s66}\right), K_{1112} = \left(\frac{1}{R^2} D_{b66} + \frac{1}{R^2} D_{s1111}\right)(-n), K_{121} = (-3D_{m101})(-\lambda), \\
 K_{122} &= \left(-\frac{1}{R^2} D_{bc62} - \frac{\gamma_0}{R^3} D_{b62} - \frac{3}{R} D_{m102} - 3\frac{\gamma_0}{R^2} D_{mc102} - \frac{1}{R^2} D_{s112} - \frac{\gamma_0}{R^3} D_{s118}\right)(n), \\
 K_{123} &= (D_{s101})(-\lambda^2) + \left(\frac{1}{R^2} D_{s112}\right)(-n^2) + \left(-\frac{1}{R^2} D_{bc62} - \frac{3}{R} D_{m102}\right), K_{124} = \left(-\frac{1}{R} D_{b61} - 3D_{mc101} + D_{s101}\right)(-\lambda),
 \end{aligned}$$

$$\begin{aligned}
K_{125} &= \left(-\frac{1}{R^2}D_{b62} - \frac{3}{R}D_{mc102} - \frac{1}{R^2}D_{s118}\right)(n), K_{126} = (D_{s107})(-\lambda^2) + \left(\frac{1}{R^2}D_{s118}\right)(-n^2) + \left(-\frac{1}{R^2}D_{b62} - 3D_{m109} - \frac{3}{R}D_{mc102}\right), \\
K_{127} &= (-3D_{m105} + 2D_{s107})(-\lambda), K_{128} = \left(-\frac{1}{R^2}D_{bc66} - \frac{3}{R}D_{m106} - \frac{1}{R^2}D_{s115} + \frac{2}{R}D_{s119}\right)(n)K_{116} = \left(\frac{1}{R^2}D_{b62} + \frac{1}{R^2}D_{s118}\right)(-n) \\
K_{129} &= (D_{s104})(-\lambda^2) + \left(\frac{1}{R^2}D_{s115}\right)(-n^2) + \left(-\frac{1}{R^2}D_{bc66} - \frac{2}{R}D_{b69} - \frac{3}{R}D_{m106} - 6D_{mc109}\right), \\
K_{1210} &= \left(-\frac{1}{R}D_{b65} - 3D_{mc105} + 3D_{s104}\right)(-\lambda), K_{1211} = \left(-\frac{1}{R^2}D_{b66} - \frac{3}{R}D_{mc106} - \frac{1}{R^2}D_{s1111}\right)(n) \\
K_{1212} &= (D_{s1010})(-\lambda^2) + \left(\frac{1}{R^2}D_{s1111}\right)(-n^2) + \left(-\frac{1}{R^2}D_{b66} - 9D_{m1010} - \frac{3}{R}D_{mc106}\right) \\
K_{15} &= 0, K_{51} = 0, K_{111} = 0, K_{111} = 0, K_{48} = 0, K_{84} = 0, K_{57} = 0, K_{75} = 0, K_{711} = 0, K_{117} = 0, K_{810} = 0, K_{108} = 0
\end{aligned}$$

D.2. Elements of Mass Matrix $M_{12 \times 12}$:

$$\begin{aligned}
M_{11} &= \bar{I}_0, M_{14} = \bar{I}_1, M_{17} = \bar{I}_2, M_{110} = \bar{I}_3; M_{22} = \left(\bar{I}_0 + \frac{2\gamma_0}{R}\bar{I}_1 + \frac{\gamma_0}{R^2}\bar{I}_2\right), M_{25} = \left(\bar{I}_1 + \frac{\gamma_0}{R}\bar{I}_2\right), \\
M_{28} &= \left(\bar{I}_2 + \frac{\gamma_0}{R}\bar{I}_3\right), M_{211} = \left(\bar{I}_3 + \frac{\gamma_0}{R}\bar{I}_4\right); M_{33} = \bar{I}_0, M_{36} = \bar{I}_1, M_{39} = \bar{I}_2, M_{312} = \bar{I}_3; M_{41} = \bar{I}_1, M_{44} = \bar{I}_2, \\
M_{47} &= \bar{I}_3, M_{410} = \bar{I}_4; M_{52} = \left(\bar{I}_1 + \frac{\gamma_0}{R}\bar{I}_2\right), M_{55} = \bar{I}_2, M_{58} = \bar{I}_3, M_{511} = \bar{I}_4; M_{63} = \bar{I}_1, M_{66} = \bar{I}_2, M_{69} = \bar{I}_3, \\
M_{612} &= \bar{I}_4; M_{71} = \bar{I}_2, M_{74} = \bar{I}_3, M_{77} = \bar{I}_4, M_{710} = \bar{I}_5; M_{82} = \left(\bar{I}_2 + \frac{\gamma_0}{R}\bar{I}_3\right), M_{85} = \bar{I}_3, M_{88} = \bar{I}_4, M_{811} = \bar{I}_5; \\
M_{93} &= \bar{I}_2, M_{96} = \bar{I}_3, M_{99} = \bar{I}_4, M_{912} = \bar{I}_5; M_{101} = \bar{I}_3, M_{104} = \bar{I}_4, M_{107} = \bar{I}_5, M_{1010} = \bar{I}_6; M_{112} = \left(\bar{I}_3 + \frac{\gamma_0}{R}\bar{I}_4\right), \\
M_{115} &= \bar{I}_4, M_{118} = \bar{I}_5, M_{1111} = \bar{I}_6; M_{123} = \bar{I}_3, M_{126} = \bar{I}_4, M_{129} = \bar{I}_5, M_{1212} = \bar{I}_6;
\end{aligned}$$

Other elements of \mathbf{M} are equal to zero.

References

- [1] Loy C, Lam K. Vibration of thick cylindrical shells on the basis of three-dimensional theory of elasticity. *Journal of sound and Vibration* 1999; 226(4): 719-37.
- [2] Hildebrand F, Reissner E, Thomas G. **Notes on the foundations of the theory of small displacements of orthotropic shells**: National Advisory Committee for Aeronautics Washington, DC; 1949.
- [3] Leissa AW. **Vibration of shells**: Scientific and Technical Information Office, National Aeronautics and Space Administration Washington, DC, USA; 1973.
- [4] Bhimaraddi A. A higher order theory for free vibration analysis of circular cylindrical shells. *International Journal of Solids and Structures* 1984; 20(7): 623-30.
- [5] Reddy J, Liu C. A higher-order shear deformation theory of laminated elastic shells. *International Journal of Engineering Science* 1985; 23(3): 319-30.
- [6] Singal R, Williams K. A theoretical and experimental study of vibrations of thick circular cylindrical shells and rings. *Journal of Vibration and Acoustics* 1988; 110(4): 533-7.
- [7] Soldatos K, Hadjigeorgiou V. Three-dimensional solution of the free vibration problem of homogeneous isotropic cylindrical shells and panels. *Journal of Sound and Vibration* 1990; 137(3): 369-84.
- [8] Kant T, Kumar S, Singh U. Shell dynamics with three-dimensional degenerate finite elements. *Computers & structures* 1994; 50(1): 135-46.
- [9] Qatu MS. Recent research advances in the dynamic behavior of shells: 1989–2000, Part 2: Homogeneous shells. *Applied Mechanics Reviews* 2002; 55(5): 415-34.
- [10] Khalili S, Davar A, Malekzadeh Fard K. Free vibration analysis of homogeneous isotropic circular cylindrical shells based on a new three-dimensional refined higher-order theory. *International Journal of Mechanical Sciences* 2012; 56(1): 1-25.

- [11] Rogers C, Knight Jr C. An axisymmetric linear/high-order finite element for filament-wound composites—I. Formulation and algorithm. *Computers & structures* 1988; 29(2): 265-71.
- [12] Krishna Murthy A, Reddy T. A higher order theory of laminated composite cylindrical shells. 1986.
- [13] Ye J, Soldatos K. Three-dimensional vibration of laminated cylinders and cylindrical panels with symmetric or antisymmetric cross-ply lay-up. *Composites Engineering* 1994; 4(4): 429-44.
- [14] Kant T, Menon M. Higher-order theories for composite and sandwich cylindrical shells with C_0 finite element. *Computers & structures* 1989; 33(5): 1191-204.
- [15] Timarci T, Soldatos K. Comparative dynamic studies for symmetric cross-ply circular cylindrical shells on the basis of a unified shear deformable shell theory. *Journal of Sound and Vibration* 1995; 187(4): 609-24.
- [16] J. C. Theory of thick laminated composite shallow shells. *PhD Thesis, The Ohio State University* 1993.
- [17] Leissa A, Chang J-D. Elastic deformation of thick, laminated composite shells. *Composite structures* 1996; 35(2): 153-70.
- [18] Qatu MS. Accurate equations for laminated composite deep thick shells. *International Journal of Solids and Structures* 1999; 36(19): 2917-41.
- [19] Lam K, Qian W. Free vibration of symmetric angle-ply thick laminated composite cylindrical shells. *Composites Part B: Engineering* 2000; 31(4): 345-54.
- [20] Icardi U, Ruotolo R. Laminated shell model with second-order expansion of the reciprocals of Lamé coefficients H_α , H_β and interlayer continuities fulfilment. *Composite structures* 2002; 56(3): 293-313.
- [21] Byon O, Nishi Y, Sato S. Optimizing lamination of hybrid thick-walled cylindrical shell under external pressure by using a genetic algorithm. *Journal of Thermoplastic Composite Materials* 1998; 11(5): 417-28.
- [22] Chandrashekhara K, Nanjunda Rao K. Approximate elasticity solution for a long and thick laminated circular cylindrical shell of revolution. *International journal of solids and structures* 1997; 34(11): 1327-41.
- [23] Ganapathi M, Patel B, Pawargi D. Dynamic analysis of laminated cross-ply composite non-circular thick cylindrical shells using higher-order theory. *International journal of solids and structures* 2002; 39(24): 5945-62.
- [24] Khare RK, Rode V, Garg AK, John SP. Higher-order closed-form solutions for thick laminated sandwich shells. *Journal of Sandwich Structures and Materials* 2005; 7(4): 335-58.
- [25] Zhen W, Wanji C. A global-local higher order theory for multilayered shells and the analysis of laminated cylindrical shell panels. *Composite Structures* 2008; 84(4): 350-61.